Failure to maternally reprogram histone methylation causes developmental delay due to germline transcription in somatic tissues

Brandon S. Carpenter[1], Teresa W. Lee[1], Caroline F. Plott[2], Jovan S. Brockett[3], Dexter A. Myrick[1], David J. Katz[1*]

[1]Department of Cell Biology, Emory University School of Medicine, Atlanta GA 30322, USA.

[2]Department of Genetics and Development, Columbia University, New York NY 10032, USA.

[3]Department of Biology, Oglethorpe University, Atlanta GA 30319, USA.

*corresponding author:
David J. Katz
Associate Professor
Department of Cell Biology
Room 443, Whitehead Biomedical Research Building
Emory University School of Medicine
Atlanta, GA 30322, USA
Phone: (404) 727-3403
djkatz@emory.edu

ABSTRACT

In *C. elegans*, the H3K36 methyltransferase, MES-4, helps establish germ cell fate by maintaining H3K36me2/3 at germline genes between generations. Previously, we showed that the H3K4me2 demethylase, SPR-5, and the H3K9 methyltransferase, MET-2, reprogram histone methylation at fertilization to prevent the ectopic expression of germline genes in somatic tissues. Together, this indicates that SPR-5 and MET-2 maternal reprogramming may antagonize MES-4 to establish germline versus soma. Here, we show that *spr-5; met-2* mutant progeny have a severe developmental delay that is associated with the ectopic maintenance of H3K36me2/3 at MES-4 targeted germline genes in somatic tissues, and the ectopic expression of these genes. We further show that the developmental delay and the ectopic expression are dependent upon MES-4. Thus, we propose that SPR-5, MET-2, and MES-4 balance inherited histone methylation to establish germline versus soma. Without this balance, the inappropriate transcription of germline genes in somatic tissues causes developmental delay.

INTRODUCTION

In multicellular organisms, developmental cell fate decisions are established by tightly controlled spatial and temporal gene expression. This pattern of gene expression can be regulated by heritable modifications on the N-terminal tails of histone proteins (Jambhekar et al., 2019). For example, methylation of lysine 4 and 36 on histone 3, (H3K4me and H3K36me) are generally associated with active transcription, whereas methylation of lysine 9 on the same histone (H3K9me) is commonly associated with transcriptional repression. These modifications are dynamically regulated by the specific

24 and tightly controlled activity of histone modifying enzymes. For instance, mono- and di-
25 methylation of lysine 4 on histone H3 (H3K4me1/2) are removed by the demethylase
26 LSD1/KDM1A (Y. Shi et al., 2004; Y.-J. Shi et al., 2005). In the nematode *C. elegans*,
27 populations of mutants lacking the LSD1 ortholog, SPR-5, become increasingly sterile over
28 ~30 generations (Katz et al., 2009). Failure to erase H3K4me2 at fertilization between
29 generations in *spr-5* mutants correlates with an accumulation of H3K4me2 and
30 spermatogenesis gene expression across 30 generations, which leads to increasing sterility
31 (Katz et al., 2009). These data demonstrate that H3K4me2 can function as an epigenetic
32 transcriptional memory. More recently, it was demonstrated that SPR-5 synergizes with
33 the H3K9me2 methyltransferase MET-2, to regulate maternal epigenetic reprogramming
34 (Kerr et al., 2014). MET-2 is the ortholog of the mammalian SETDB1. Progeny of mutants
35 lacking both SPR-5 and MET-2 become completely sterile in a single generation and display
36 synergistic increases in both H3K4me2 and candidate germline gene expression in somatic
37 tissues (Kerr et al., 2014). Together this work supports a model in which SPR-5 and MET-2
38 are maternally deposited into the oocyte, where they reprogram histone methylation to
39 prevent somatic expression of germline genes.
40 Following fertilization, the *C. elegans* embryo separates germline versus somatic
41 lineages progressively through a series of asymmetric divisions (Strome, 2005). To
42 accomplish this, transcription factors coordinate with multiple histone modifications.
43 Maternal deposition of PIE-1, a germline specific protein that asymmetrically segregates
44 into germline blastomeres (P lineage cells), maintains the fate of germ cells by inhibiting
45 POL-II elongation and preventing the ectopic expression of somatic genes (Batchelder et al.,
46 1999; Mello et al., 1992; Seydoux et al., 1996). In the absence of transcription in the

germline, the maternally provided H3K36me2/3 methyltransferase, MES-4, binds to a subset of germline genes that were previously expressed in the parental germline (Furuhashi et al., 2010; Rechtsteiner et al., 2010). These germline genes are recognized by MES-4 via H3K36me2/3 that was added in the parental germline by the transcription-coupled H3K36me2/3 methyltransferase, MET-1 (Kreher et al., 2018). MES-4 maintains H3K36me2/3 at these genes in the early embryo in a transcriptionally independent manner. Without maternally deposited MES-4, the germline cannot properly proliferate and animals are sterile (Capowski et al., 1991; Garvin et al., 1998). For the remainder of this study, we will refer to these MES-4 targeted genes as MES-4 germline genes, and the process through which MES-4 maintains these genes for re-activation in the primordial germ cells of the offspring, as bookmarking.

In addition to providing transcriptional memory of germline genes between generations in the germline, histone methylation has been implicated in repressing germline transcription in somatic tissues. Recent work in *C. elegans* has shown that a subset of germline genes have H3K9me2 enrichment at their promoters in somatic tissues (Rechtsteiner et al., 2019). Loss of LIN15B, a transcriptional repressor that is a putative member of the DREAM complex, reduces the enrichment of H3K9me2, leading to the ectopic accumulation of H3K36me3 at gene bodies in somatic tissues (Rechtsteiner et al., 2019). These data implicate H3K9me2 in germline gene repression in somatic tissues and raise the possibility that H3K9me2 antagonizes MES-4. As mentioned earlier, previous work suggests that H3K9me2 also functions antagonistically to H3K4me2 (Kerr et al., 2014). However, whether the maternal histone modifying enzymes SPR-5 and MET-2 coordinate with MES-4 to ensure the proper inheritance of histone methylation and the

70 proper specification of germline versus soma remains unclear. To address this question, we
71 examined somatic development in progeny deficient in SPR-5 and MET-2 maternal
72 reprogramming. We find that *spr-5; met-2* double mutant progeny (hereafter referred to as
73 *spr-5; met-2* progeny) display a severe developmental delay that is rescued by removing
74 MES-4. In addition, H3K36me3 ectopically accumulates at germline genes in the somatic
75 tissues of *spr-5; met-2* progeny. This accumulation correlates with the ectopic expression of
76 MES-4 germline genes and is rescued by knocking down MES-4 activity. These data
77 demonstrate that the ectopic expression of MES-4 targeted germline genes in somatic
78 tissues causes a developmental delay. We propose a model where SPR-5 and MET-2
79 function together during maternal reprogramming to restrict MES-4 dependent
80 bookmarking of germline genes in somatic tissues, thereby ensuring proper specification of
81 germline versus somatic cell fates.
82
83 **RESULTS**
84 **Loss of *spr-5* and *met-2* causes developmental delay**
85 Previous work from our lab demonstrated that progeny from *spr-5; met-2* mutants
86 express germline genes in somatic lineages (Kerr et al., 2014). To examine how
87 misexpression of germline genes in somatic tissues affects somatic development, we
88 synchronized embryos laid by N2, *spr-5*, *met-2*, and *spr-5; met-2* mutant hermaphrodites
89 and monitored their development from hatching to adults. By 72 hours past the
90 synchronized lay, all N2 progeny (469/469), most of the *spr-5* progeny (363/385), and
91 many of *met-2* progeny (386/450) were fertile adults (Figure 1 A, B, C, and E, S1A-C). In
92 contrast, *spr-5; met-2* progeny displayed a severe developmental delay. By 72 hours past

93 the synchronized lay, none of the progeny (0/463) had reached adulthood (Figure 1 D, E;
94 and S1D). The majority of *spr-5; met-2* progeny (371/463) resembled L2 larvae at 72 hours,
95 while a smaller percentage of the population developed to later larval stages (42/463)
96 (Table S1). By seven days post synchronized lay, a small number of *spr-5; met-2* progeny
97 (35/876) developed into adults and the majority (31/35) of these adults displayed
98 protruding vulva (Pvl) (Figure S1E-G). All 35 of the *spr-5; met-2* mutant progeny that
99 developed to adulthood were sterile.
100
101 **MES-4 germline genes are ectopically expressed in *spr-5; met-2* mutant soma**
102 Previously we showed that H3K4me2 is synergistically increased in *spr-5; met-2*
103 progeny compared to *spr-5* and *met-2* single mutant progeny, and that this increase in
104 H3K4me2 correlates with a synergistic increase in candidate germline gene expression in
105 somatic tissues (Kerr et al., 2014). To test the extent to which germline genes are
106 ectopically expressed in somatic tissues, we examined somatic expression genome-wide.
107 To do this, we performed RNA-seq on *spr-5; met-2* L1 progeny compared to N2 (wild-type)
108 L1 progeny. We chose to perform this analysis on L1 larvae because this stage immediately
109 precedes the L2 larval delay that we observe in *spr-5; met-2* progeny (see Figure 1A, D). In
110 addition, L1 larvae are composed of 550 somatic cells and 2 germ cells. Therefore, L1
111 larvae are primarily composed of somatic tissue. As a control, we also performed RNA-seq
112 on L1 progeny from *spr-5* and *met-2* single mutants that were isolated from early
113 generation animals (within 1-5 generations). These generations are well before the onset
114 of sterility that we previously reported (Katz et al., 2009; Kerr et al., 2014). We identified
115 778 differentially expressed transcripts in *spr-5; met-2* progeny compared to N2 (Figure

116 S2A-B, Figure S3C, F, and Table S2), many of which also overlap with genes differentially
117 expressed in *spr-5* (159/413) and *met-2* single mutants (113/343) compared to N2.
118 (Figure S2A-B, Figure S3A, B, S3D, E, and Table S2). Gene Set Enrichment Analysis (GSEA)
119 did not identify any categories of genes misexpressed in the *spr-5* or *met-2* single mutants.
120 However, GSEA revealed that genes differentially expressed in *spr-5; met-2* progeny were
121 significantly enriched (based on Combined Score, (Chen et al., 2013)) for biological
122 processes and cellular components characteristic of the germline; including meiosis, P-
123 granules and negative regulation of the cell cycle (Figure S2C-D). Many of the genes
124 involved in these processes are expressed in the germline of the parental generation,
125 bound by the H3K36 methyltransferase MES-4 in the early embryo, and marked by
126 H3K36me2/3, independent of POL-II (Rechtsteiner et al., 2010). As a result, we were
127 interested in the potential overlap with MES-4 targeted genes (referred to as MES-4
128 germline genes). Rechtsteiner and colleagues identified 214 MES-4 germline genes
129 (Rechtsteiner et al., 2010). 17 of these genes are pseudogenes that we were unable to
130 convert from Ensembl transcript IDs to RefSeq mRNA accession, and another gene was
131 duplicated, so we removed those genes from our analysis. This leaves 196 MES-4 germline
132 genes. We reasoned that the absence of SPR-5 and MET-2 reprogramming may cause
133 germline genes to be aberrantly targeted by MES-4 in the soma, leading to ectopic
134 expression. To investigate this possibility, we examined the overlap between differentially
135 expressed genes in *spr-5; met-2* L1 progeny and MES-4 germline genes. Out of 196 MES-4
136 germline genes, 34 overlapped with genes up-regulated in *spr-5; met-2* progeny compared
137 to N2 (hypergeometric test (P-value < 4.34e-20, Figure 2A), while zero overlapped with
138 genes down-regulated in *spr-5; met-2* progeny compared to N2 (Figure 2B). In addition,

139 when we compared the log2 fold change (FC) in expression of all of the MES-4 genes in *spr-*
140 *5*, *met-2*, and *spr-5; met-2* mutant progeny compared to N2, we observed that 108 of the
141 MES-4 germline genes are synergistically increased in *spr-5; met-2* progeny compared to
142 single mutant progeny (Figure 2C and Table S3). This analysis included only 176 out of the
143 196 MES-4 germline genes because the remaining 21 genes do not have an expression
144 value in one or more of the data sets (*spr-5*, *met-2,* or *spr-5; met-2*).
145 To confirm that MES-4 germline genes are somatically expressed in *spr-5; met-2* L1
146 progeny, we performed single molecule fluorescent *in situ* hybridization (smFISH) on two
147 MES-4 germline targets, *htp-1* and *cpb-1* (Figure 3). Both of these genes were amongst the
148 genes that were ectopically expressed in *spr-5; met-2* L1 progeny compared to N2 L1
149 progeny. In N2 L1 larvae, *htp-1* (Figure 3A-C, insets) and *cpb-1* (Figure 3G-I, insets) were
150 restricted to the two primordial germ cells, Z2 and Z3. In contrast, in *spr-5; met-2* progeny
151 *htp-1* was ectopically expressed throughout the soma (Figure 3D-F), similar to what we
152 observe with the ubiquitously expressed subunit of RNA polymerase II, *ama-1* (Figure S4A-
153 L), which was unchanged in our RNA-seq analysis. *cpb-1* was also ectopically expressed,
154 though the ectopic expression was not ubiquitous as it is in *htp-1* (Figure 3J, L).
155
156 **MES-4 dependent germline genes display ectopic H3K36me3 in *spr-5; met-2* mutants**
157 To test whether MES-4 germline genes that are ectopically expressed in the soma of
158 *spr-5; met-2* progeny also ectopically maintain H3K36me3, we performed H3K36me3 ChIP-
159 seq. Similar numbers of H3K36me3 peaks were called between N2 (replicate 1 = 5507 and
160 replicate 2 = 3878) and *spr-5; met-2* (replicate 1 = 5886 and replicate 2 = 1938) progeny,
161 with most of the peaks overlapping between replicates (Figure S5Q-R). MES-4 germline

162 genes have low levels of H3K36me3 in N2 L1 progeny. However, compared to N2 L1
163 progeny, *spr-5; met-2* L1 progeny displayed increased enrichment for H3K36me3 across
164 the gene bodies at MES-4 germline genes (Figure 4A, B; Figure S5A, B). For example, the
165 MES-4 germline genes *cpb-1*, *T05B9.1, Y18D10A.11*, and *fbxa-101,* that are ectopically
166 expressed in our RNA-seq analysis, showed increased levels of H3K36me3 in *spr-5; met-2*
167 progeny (Figure 4J-M; Figure S5J-M) compared to N2 progeny (Figure 4 C-F; Figure S5C-F).
168 As a control, we examined H3K36me3 enrichment at *ceh-13*, a gene enriched in
169 hypodermal and ventral nerve chord in L1 progeny (Figure 4G, N; Figure S5G, N), *ama-1*, a
170 subunit of RNA polymerase II that is expressed ubiquitously (Figure 4H, O; Figure S5H, O),
171 and *act-1*, a ubiquitously expressed actin related protein (Figure 4I, P; Figure S5I, P). These
172 control genes displayed similar H3K36me3 enrichment in both *spr-5; met-2* and N2 L1
173 progeny (compare Figure 4N-P and Figure S5N-P to Figure 4G-I and Figure S5G-I,
174 respectively).
175
176 **MES-4 germline genes display H3K9me2 at their promoter peaks**
177 Recent work discovered that a subset of germline specific genes contain H3K9me2
178 peaks at their promoters in N2 L1 progeny (Rechtsteiner et al., 2019). This finding
179 implicates H3K9me2 enrichment at promoters of germline genes as being a critical
180 component for repressing germline genes in somatic tissues. If SPR-5 and MET-2 are
181 functioning to prevent MES-4 germline genes from being ectopically expressed in somatic
182 tissues, we would expect MES-4 germline genes that are ectopically expressed in the
183 somatic tissues of *spr-5; met-2* progeny to be targeted by H3K9 methylation in these
184 tissues. To examine this possibility, we re-analyzed L1 H3K9me2 Chip-seq data from

185 Rechsteiner et al. 2019 (Rechtsteiner et al., 2019). This re-analysis shows that many of the
186 MES-4 germline genes were enriched for H3K9me2 at their promoters (Figure S6A),
187 including the majority of MES-4 germline genes that are ectopically expressed in the soma
188 of *spr-5; met-2* progeny (Figure S6B). For example, the MES-4 germline genes *cpb-1*,
189 *T05B9.1*, *Y18D10A.11*, and *fbxa-101*, that accumulate ectopic H3K36me3 and were
190 ectopically expressed in the somatic tissues of *spr-5; met-2* progeny, have H3K9me2 peaks
191 at their promoters (Figure 6SC-F). In contrast, control genes, *ceh-13*, *ama-1*, and *act-1*, that
192 are not expressed ectopically in the somatic tissues of *spr-5; met-2* progeny were not
193 enriched for H3K9me2 at their promoters (Figure 6SG-I).
194

195 **Knocking down MES-4 rescues ectopic expression of germline genes in *spr-5; met-2***
196 **mutant soma**

197 To test whether the ectopic expression of MES-4 germline genes in *spr-5; met-2*
198 progeny is dependent on the ectopic H3K36me3, we examined whether the expression of
199 these genes was dependent upon MES-4. We performed quantitative real-time PCR (qRT-
200 PCR) on L1 progeny from *spr-5; met-2* hermaphrodites fed control (L4440) RNAi versus
201 *mes-4* RNAi (Figure 5). For this analysis, we selected candidate MES-4 germline genes that
202 were ectopically expressed and displayed an ectopic H3K36me3 peak in *spr-5; met-2* L1
203 progeny compared to N2 L1 progeny. Consistent with our RNA-seq analysis, all nine of the
204 candidate MES-4 germline genes that we examined were ectopically expressed >2 fold in
205 *spr-5; met-2* L1 progeny compared to control (Figure 5). Strikingly, the ectopic expression
206 of the nine MES-4 candidate germline genes was dependent upon MES-4. Nine out of nine
207 of these genes were significantly decreased in L1 progeny from *spr-5; met-2*

208 hermaphrodites treated with *mes-4* RNAi (Figure 5; p-value < 0.001), and all but one
209 (*T05B9.1*) were reduced to levels that were similar to N2 L1 progeny.
210
211 **Knocking down MES-4 rescues developmental delay in *spr-5; met-2* progeny**
212 To test whether the developmental delay phenotype that we observe in *spr-5; met-2*
213 progeny is also dependent on the ectopic expression of MES-4 germline genes, we fed *spr-5;*
214 *met-2* hermaphrodites *mes-4* RNAi and monitored their progeny for 72 hours after a
215 synchronized lay. If the developmental delay is dependent upon the ectopic expression of
216 MES-4 germline genes, it should be suppressed when this ectopic expression is eliminated
217 via *mes-4* RNAi. 72 hours after a synchronized lay, all of the N2 control progeny from
218 hermaphrodites fed either L4440 control (1089/1089) or *mes-4* (1102/1102) RNAi were
219 adults (Figure 6A, B, I). Also, consistent with our previous observations, all but one of the
220 *spr-5; met-2* mutant progeny (729/730) from hermaphrodites fed control RNAi remained
221 in the L2-L3 larval stages (Figure 6E, I). In contrast, most of *spr-5; met-2* progeny
222 (569/618) from hermaphrodites fed *mes-4* RNAi developed to adults (Figure 6F, I). Though
223 as expected, these animals remained sterile due to the *mes-4* RNAi preventing any germline
224 formation.
225 MET-1 mediates transcription-coupled H3K36me3 in the adult germline and in later
226 stage transcriptionally active embryos (Furuhashi et al., 2010; Kreher et al., 2018;
227 Rechtsteiner et al., 2010). If the ectopic somatic expression of MES-4 germline genes is
228 caused by the transcription independent maintenance of H3K36me3 via MES-4, we would
229 expect the developmental delay to be independent of MET-1. To determine whether the
230 developmental delay phenotype in *spr-5; met-2* progeny is dependent on MET-1, we

231 monitored the development of progeny from *spr-5; met-2* hermaphrodites fed *met-1* RNAi.
232 In contrast to the suppression that we observed upon *mes-4* RNAi, *met-1* RNAi had no
233 effect. None of the *spr-5; met-2* mutant progeny (0/573) from hermaphrodites fed *met-1*
234 RNAi developed to adults, and these animals were indistinguishable from *spr-5; met-2*
235 progeny fed control RNAi (Figure 6G, I). Additionally, *met-1* RNAi itself had no effect on
236 developmental delay, as nearly all of the N2 progeny (715/721) from hermaphrodites fed
237 *met-1* RNAi developed to adults (Figure 6C, I).
238
239 **Knocking down SET-2 rescues *spr-5; met-2* developmental delay**
240 If the developmental delay of *spr-5; met-2* mutants is caused by ectopic H3K4me2
241 driving the expression MES-4 germline genes in somatic tissues, we would expect the
242 developmental delay of *spr-5; met-2* progeny to be dependent upon the H3K4
243 methyltransferase, SET-2. To test this, we monitored the development of progeny of *spr-5;*
244 *met-2* hermaphrodites fed *set-2* RNAi. Identical to N2 progeny from hermaphrodites fed
245 control RNAi, *set-2* RNAi had no effect on the development of wild-type animals, as all of
246 the N2 progeny from hermaphrodites fed *set-2* RNAi developed to adults (1114/1114)
247 (Figure 6D, I). However, in contrast to *spr-5; met-2* progeny fed control RNAi that were
248 developmentally delayed, most of the progeny from *spr-5; met-2* hermaphrodites fed *set-2*
249 RNAi developed to adults (347/384) (Figure 6H, I).
250
251 ***spr-5; met-2* progeny acquire transgene silencing in somatic tissues**
252 The somatic expression of MES-4 germline genes involved in germline transgene
253 silencing (Figure S2C-D) raises the possibility that the somatic tissues in *spr-5; met-2*

254 progeny may acquire the ability to silence transgenes, a function normally restricted to
255 germline cells. To test this, we examined the somatic expression of an extrachromosomal
256 multicopy *let-858* transgene that is normally silenced in the germline by both
257 transcriptional and posttranscriptional germline silencing mechanisms (Kelly and Fire,
258 1998). This analysis was performed in *spr-5; met-2* mutant L2 larvae that were undergoing
259 developmental delay. In N2, most of the L2 progeny (117/132) expressed ubiquitous high
260 levels of LET-858::GFP throughout the entire soma (Figure 7A, B, and K), while the
261 remaining progeny (15/132) expressed what we describe as a "faint" level of expression
262 (Figure 7C, D, and K). In contrast, almost none of the *spr-5; met-2* L2 progeny (2/87)
263 displayed high level of transgene expression that is comparable to the high level seen in
264 most N2 progeny (Figure 7E, F, and K). Instead, the majority of *spr-5; met-2* progeny
265 (64/87) had faint LET-858::GFP expression that is comparable to the faint expression
266 observed in N2 progeny (Figure 7G, H, and K). The remaining 21 *spr-5; met-2* progeny had
267 no LET-858::GFP expression. Because less than 50% of progeny inherited the *let-858*
268 transgene, we normalized the percentage of progeny scored as "off" for LET-858::GFP to
269 presence of the *let-858* transgene based on genotyping for *gfp* (see methods). For N2, all of
270 the 60 L2 progeny that were scored as "off" failed to inherit the *let-858* transgene,
271 indicating that the transgene is never silenced in N2 progeny (data not shown). However,
272 for *spr-5; met-2* L2 progeny, eight out of 50 progeny that were scored as "off" inherited the
273 *let-858* transgene indicating that the *let-858* transgene can be completely silenced in some
274 *spr-5; met-2* progeny. After normalization for the transgene inheritance, we observed that
275 21/87 of *spr-5; met-2* progeny displayed no visible expression of the LET-858::GFP
276 transgene (Figure 7I, J, and K).

277
278 **DISCUSSION**

279 **Maternal regulation of inherited histone methylation contributes to the specification**
280 **of germline versus soma**

281 SPR-5 and MET-2 are thought to act maternally to reprogram histone methylation
282 and prevent the transcriptional "baggage" of the parental germline from being
283 inappropriately transmitted to the offspring (Kerr et al., 2014). In this study, we find that
284 the lack of SPR-5 and MET-2 maternal reprogramming led to a severe developmental delay.
285 This developmental delay was associated with the ectopic expression of MES-4 germline
286 genes in somatic tissues. This finding raises the possibility that SPR-5 and MET-2
287 reprogramming blocks the ectopic expression of MES-4 germline genes by preventing the
288 accumulation of MES-4 dependent H3K36me3 at a subset of germline genes in somatic
289 tissues. Consistent with this, most of the MES-4 germline genes were overexpressed in *spr-*
290 *5; met-2* mutants. Using smFISH, we also defined the somatic expression of two ectopically
291 expressed MES-4 germline genes, *htp-1* and *cpb-1*. While *htp-1* mRNA was ectopically
292 detected in many somatic tissues, the ectopic expression of *cpb-1* mRNA was more
293 restricted, suggesting that the extent of ectopic expression is dependent upon the locus.

294 To directly test whether SPR-5 and MET-2 reprogramming prevents the
295 accumulation of MES-4 dependent H3K36me3 at germline genes in the somatic tissues of
296 *spr-5; met-2* progeny, we performed H3K36me3 ChIP-seq. MES-4 germline genes
297 accumulated ectopic H3K36me3 in the soma of *spr-5; met-2* progeny compared to the soma
298 of N2 progeny. This suggests that without SPR-5 and MET-2 reprogramming, MES-4
299 ectopically maintains H3K36me3 at these genes in somatic tissues. Importantly, a low level
300 of H3K36me3 was detected at germline genes in the somatic tissues of N2 progeny. It is

301 unclear why there is a low level of H3K36me3 normally in somatic tissues in N2 animals.
302 Nevertheless, this indicates that an increased level of H3K36me3 is necessary to cause
303 ectopic transcription.

304 If the developmental delay of *spr-5; met-2* mutant progeny is caused by the ectopic
305 maintenance of H3K36me3, and the subsequent expression of MES-4 germline genes, then
306 the ectopic expression of germline genes and the developmental delay should be
307 dependent upon MES-4. Indeed, we find that the removal of MES-4 rescued both the ectopic
308 transcription of MES-4 germline genes in the soma of *spr-5; met-2* progeny, and the
309 developmental delay. Taken together, these results suggest that the developmental delay in
310 *spr-5; met-2* progeny is caused by the ectopic expression of MES-4 germline genes. In
311 contrast, removing the transcriptionally coupled H3K36me3 methyltransferase, MET-1, did
312 not rescue the developmental delay. Thus, the developmental delay that we observe in *spr-*
313 *5; met-2* progeny is only dependent on transcriptionally independent H3K36me3.

314 Our data support the following model for how maternal reprogramming by SPR-5
315 and MET-2 facilitates proper specification of germline versus soma. In the germline,
316 transcriptional elongation is blocked by PIE-1, which segregates to germline blastomeres
317 during embryogenesis (Batchelder et al., 1999; Mello et al., 1992; Seydoux et al., 1996)
318 (Figure 8A, B). In the soma of the early embryo, there is also very little transcription,
319 because the bulk of zygotic transcription does not begin until approximately the 60 cell
320 stage, just prior to when the primordial germ cells Z2 and Z3 are specified (Sulston et al.,
321 1983). Thus, in *C. elegans,* germline versus soma is largely specified without transcription.
322 During normal maternal reprogramming, SPR-5 and MET-2 are deposited into the oocyte,
323 where at fertilization they cooperate to remove H3K4me2 and add H3K9me2 to genes that

324 were expressed previously in the parental germline (Kerr et al., 2014) (Figure 8A). This
325 facilitates the transition from active chromatin to repressed chromatin. Genes
326 epigenetically reprogrammed by SPR-5 and MET-2 include ubiquitously expressed genes
327 and germline expressed genes, including MES-4 germline genes. The MES-4 germline genes
328 are subsequently targeted by the transcription independent H3K36 methyltransferase
329 MES-4 to maintain H3K36me3 in the germ lineage during embryogenesis (Figure 8A, B).
330 This H3K36 methylation bookmarking antagonizes the repression caused by the erasure of
331 H3K4me2 and the addition of H3K9me2. Without the transcription independent
332 maintenance of inherited H3K36 methylation from the mother to antagonize this
333 repression, the germline fails to proliferate and animals are sterile (Capowski et al., 1991;
334 Garvin et al., 1998). This is presumably because germline genes that are targeted by MES-4
335 fail to reactivate, though this has not yet been demonstrated. In contrast, without SPR-5
336 and MET-2 repression, the failure to add H3K9me2 as well as the inappropriate retention
337 of H3K4me2 results in a chromatin environment that is permissive for the ectopic
338 maintenance of H3K36me3 in the soma (Figure 8B). This causes germline genes to be
339 inappropriately expressed in somatic tissues and results in a severe developmental delay
340 (Figure 8B).Thus, we propose that SPR-5, MET-2 and MES-4 carefully balance the
341 inheritance of histone methylation from the parental germline to ensure the proper
342 specification of germline versus soma in the progeny.
343 The model that we have proposed makes the following two predictions. First, MES-4
344 germline genes should normally be targeted for silencing by H3K9me2 in somatic tissues. It
345 has recently been shown that a subset of germline specific genes contain H3K9me2 at their
346 promoters in L1 larvae, and that these peaks are lost or reduced in the absence of LIN15B

347 (Rechtsteiner et al., 2019). We re-examined the H3K9me2 ChIP-seq dataset from this work
348 and found that the MES-4 germline genes that are ectopically expressed in the somatic
349 tissues of *spr-5; met-2* progeny also displayed unique H3K9me2 promoter peaks. This
350 confirms that these genes are normally repressed by H3K9me2 in somatic tissues.
351 Additionally, the requirement for LIN15B in maintaining somatic H3K9me2 indicates that
352 the DREAM complex may function to reinforce the expression pattern established by SPR-5
353 and MET-2. Interestingly, the MEC complex members MEP-1 and LET-418 have also been
354 implicated in repressing germline genes in somatic tissues (Passannante et al., 2010;
355 Unhavaithaya et al., 2002). This raises the possibility that the expression pattern
356 established by SPR-5 and MET-2 may also be reinforced by the MEC complex. The second
357 prediction from our model is that the developmental delay in *spr-5; met-2* progeny should
358 be dependent upon the activity of the H3K4 methyltransferase complex. Consistent with
359 our model, we find that knocking down SET-2, the H3K4me1/2 methyltransferase
360 component of the COMPASS complex, also rescued the developmental delay that we
361 observe in *spr-5; met-2* progeny. These findings suggest that the inheritance of ectopic
362 H3K4 methylation is required for the ectopic accumulation of MES-4 dependent
363 H3K36me3, and the subsequent ectopic expression of MES-4 germline genes in somatic
364 tissues of *spr-5; met-2* progeny.
365

366 **A new paradigm for how an ectopic transcriptional program interferes with**
367 **development**

368 Our model explains how H3K36me3 is inappropriately maintained and drives the
369 ectopic expression of MES-4 germline genes in somatic tissues, but how does the ectopic

370 expression of germline genes interfere with somatic tissues to cause developmental delay?
371 One possibility is that the ectopic expression of MES-4 germline genes causes the soma to
372 take on germline character. To begin to address this, we asked whether *spr-5; met-2* double
373 mutants can silence an extrachromosomal array in somatic tissues. The silencing of
374 extrachromosomal arrays is normally restricted to the germline. However, we find that *spr-*
375 *5; met-2* progeny acquired some ability to silence an extrachromosomal multicopy array in
376 somatic cells. Intriguingly, in our RNA-seq we detected the ectopic expression of RNA-
377 dependent RNA polymerase genes (e.g. *rrf-1* and *gld-2*) as well as genes involved in the
378 RNAi effector complex in *spr-5; met-2* mutants (e.g. *hrde-1* and *ppw-1*) Thus, it is possible
379 that the somatic silencing of the transgene in *spr-5; met-2* mutants is due to the induction of
380 the germline small RNA pathway. Regardless, the silencing of the extrachromosomal
381 multicopy array suggests that the somatic tissues in *spr-5; met-2* progeny make functional
382 proteins that can perform some germline functions. We propose that either the ectopic
383 germline transcription, or an ectopic germline function resulting from this ectopic
384 transcription, interferes with the ability of somatic cells to properly read out the correct
385 somatic transcriptional program. This background noise delays the proper adoption of cell
386 fate, leading to an overall delay in the development of the tissue. Normally in L1 larvae, the
387 primordial germ cells Z2 and Z3 are arrested at the G2/M checkpoint (Fukuyama et al.,
388 2006). In our RNA-seq, we detected the ectopic expression of genes involved in the
389 negative regulation of proliferation and the cell cycle, as well as G2/M checkpoint genes.
390 Thus, it is also possible that ectopic expression of germline genes normally expressed only
391 in Z2 and Z3 contributes to the developmental delay through the ectopic activation of
392 germline cell cycle control.

393

394 **Conservation of maternal epigenetic reprogramming between invertebrates and**

395 **vertebrates**

396 It is possible that the maternal regulation of histone methylation by SPR-5, MET-2

397 and MES-4 is conserved in mammals. Along with the Heard lab, we previously

398 demonstrated that progeny from mice that maternally lack the vertebrate SPR-5 homolog,

399 KDM1A/LSD1, ectopically express oocyte genes and die at the two-cell stage (Ancelin et al.,

400 2016; Wasson et al., 2016). Similarly, maternal loss of the MET-2 ortholog SEDB1 or the

401 MES-4 ortholog NSD1 in mice results in early embryonic lethality (J. Kim et al., 2016;

402 Rayasam et al., 2003). Together these results underscore the developmental importance of

403 properly regulating histone methylation between generations and raise the possibility that

404 the mechanism we have uncovered is conserved in mammals. The model that we have

405 proposed may also help explain how patients harboring mutations in histone modifying

406 enzymes suffer from certain symptoms. Recent genome sequencing of patients has

407 revealed that several neurodevelopmental disorders are caused by mutations in histone

408 modifying enzymes (extensively reviewed by (J.-H. Kim et al., 2017). These include: several

409 patients with mutations in the human ortholog of *spr-5, Lsd1* (Chong et al., 2016; Tunovic et

410 al., 2014) , as well as Kabuki Syndrome, caused by mutations in the H3K36

411 methyltransferase SETD2 (Xu et al., 2019), and the H3K27 demethylase KDM6A (Lederer et

412 al., 2012), and Sotos syndrome, caused by mutations in the H3K36 methyltransferase NSD1

413 (Kurotaki et al., 2002). Similar to what we observed in *spr-5; met-2* mutant progeny, many

414 of these human patients suffer from global developmental delay. Based on our data, it is

415 possible that the developmental delay in these patients may be caused by the failure to

416 properly regulate histone methylation during critical developmental transitions. This could
417 result in the ectopic expression of a developmental program in an inappropriate tissue,
418 leading to background noise and developmental delay.
419

420 **MATERIALS AND METHODS**

421 **Strains.** All *Caenorhabditis elegans strains* were grown and maintained at 20° C under
422 standard conditions, as previously described (Brenner, 1974). The *C. elegans spr-5*
423 *(by101)(I)* strain was provided by R. Baumeister. The N2 Bristol wild-type (WT) strain was
424 provided by the *Caenorhabditis* Genetics Center. The *met-2 (n4256)(III) strain* was provided
425 by R. Horvitz. The *hT2 [bli-4(e937)let-?(q782)qls48] (I;III)* balancer strain was used to
426 maintain *spr-5 (by101)(I); met-2 (n4256)(III)* double-mutant animals as heterozygotes.
427 Because the *hT2 [bli-4(e937)let-?(q782)qls48](I;III)* balancer allele does not extend
428 completely to the *spr-5* locus on chromosome I, the F0 animals used to generate F1 *spr-5;*
429 *met-2* progeny were cloned out and genotyped to confirm the presence of the *spr-5*
430 *(by101)(I)* allele. For genotyping, single animals were picked into 5-10ul of lysis buffer
431 (50mM KCl, 10mM Tris-HCl (pH 8.3), 2.5mM $MgCl_2$, 0.45% NP-40, 0.45% Tween-20, 0.01%
432 gelatin) and incubated at 65°C for 1 hour followed by 95°C for 30 minutes. PCR reactions
433 were performed with AmpliTaq Gold (Invitrogen) according to the manufacturer's protocol
434 and reactions were resolved on agarose gels (see Table S4 for primer sequences). Before
435 completing this study we acquired the FX30208 *tmC27 [unc-75(tmls1239*)](I) from the
436 *Caenorhabditis* Genetics Center that completely covers the *spr-5* locus on chromosome I.
437 The *qC1 [qls26 (lag2::GFP + rol-6(su1006)](III)* strain was obtained from W. Kelly and
438 crossed to *met-2 (n4256)(III)* to maintain *met-2(n4256)(III)* as heterozygotes. The *spr-5*

439 *(by101)(I)/tmC27[unc-75(tmls1239)](I); met-2 (n4256) (III)*/qC1 [qls26 (lag2::gfp+ rol-
440 6(su1006))](III) strain was then re-created for this study to maintain *spr-5 (by101)(I);*
441 *met-2 (n4256)(III)* double-mutant animals as balanced heterozygotes. The LET-858::GFP
442 (*pha-1*(e2123ts)(III); *let-858::gfp* (ccEx7271)) (Kelly and Fire, 1998) transgenic strain used
443 in somatic transgene silencing assays was acquired from W. Kelly.
444 **Scoring developmental delay.** *C. elegans* adult hermaphrodites were allowed to lay
445 embryos for 2-4 hours and then removed in order to synchronize the development of
446 progeny. Progeny were then imaged and scored for development to the adult stage at
447 either 72 hours or seven days after synchronized lay, depending on the experiment.
448 **RNA sequencing and analysis.** Total RNA was isolated using TRIzol reagent (Invitrogen)
449 from 200-250 starved L1 larvae born at room temperature (21°C - 22°C) overnight in M9
450 Buffer. Due to difficulty in isolating large numbers of *spr-5; met-2* double-mutant progeny
451 from the *hT2 [bli-4(e937)let-?(q782)qls48](I;III)* balancer strain, we submitted total RNA to
452 the Genomic Services Laboratory (GSL) (HudsonAlpha, Huntsville, Alabama) for low input
453 RNA-seq services. This service utilizes the Ovation RNA-Seq System V2 kit (Nugen) for
454 initial RNA amplification prior to library preparation and sequencing (Illumina HiSeq v4,
455 50bp paired-end reads). For each genotype, 2 biological replicates were obtained.
456 Sequencing reads were checked for quality using FastQC (Wingett and Andrews, 2018),
457 filtered using Trimmomatic (Bolger et al., 2014), and remapped to the *C. elegans*
458 transcriptome (ce10, WS220) using HISAT2 (D. Kim et al., 2015). Read count by gene was
459 obtained by FeatureCounts (Liao et al., 2014) . Differentially expressed transcripts
460 (significance threshold p-value < 0.05) were determined using DESEQ2 (v.2.11.40.2) (Love
461 et al., 2014). Transcripts per million (TPM) values were calculated from raw data obtained

462 from FeatureCounts output. Subsequent downstream analysis was performed using R with
463 normalized counts and p-values from DESEQ2 (v.2.11.40.2). Heatmaps were produced
464 using the ComplexHeatmap R Package (Gu et al., 2016). Data was scaled and hierarchical
465 clustering was performed using the complete linkage algorithm. In the linkage algorithm,
466 distance was measured by calculating pairwise distance. Volcano plots were produced
467 using the EnhancedVolcano package (v.0.99.16). Additionally, Gene Ontology (GO) Pathway
468 analysis was performed using the online platform WormEnrichr (Chen et al., 2013;
469 Kuleshov et al., 2016). Custom R-scripts are available upon request. An additional heatmap
470 comparison of differentially expressed genes between *spr-5*, *met-2*, and *spr-5; met-2*
471 progeny compared to N2 progeny was generated in Microsoft Excel using Log2 fold change
472 values from the DESEQ2 analysis. Because transcript isoforms were ignored, we discuss the
473 data in terms of "genes expressed" rather than "transcripts expressed".
474 **Chromatin immunoprecipitation sequencing and analysis.** Chromatin
475 immunoprecipitation (ChIP) experiments were performed as described by Katz and
476 colleagues (Katz et al., 2009). Briefly, 600 starved L1 larvae born at room temperature
477 (21°C - 22°C) overnight in M9 Buffer were collected, frozen in liquid nitrogen, and stored at
478 -80°C prior to homogenization. Frozen pellets were disrupted by a glass Dounce
479 homogenizer, fixed with formaldehyde (1% final concentration), and quenched with
480 glycine. ChIP samples were processed with a Chromatin Immunoprecipitation Assay Kit
481 (Millipore), according to manufacturer's instructions. Samples were sonicated using a
482 Diagenode Bioruptor UCD-200 at 4°C on the "high" setting for a total of 30min with a cycle
483 of 45sec on and 15sec off. A total of 12.5µL (5 ug) H3K36me3 antibody (cat. 61021; Active
484 motif) was used for immunoprecipitation. The Genomic Services Laboratory (GSL)

485 (HudsonAlpha, Huntsville, Alabama) performed library preparation and sequencing
486 (Illumina HiSeq v4, 50bp single-end reads). Reads were checked for quality using FastQC
487 (Wingett and Andrews, 2018) and remapped to the *C. elegans* transcriptome (ce10, WS220)
488 using Bowtie2 (Langmead and Salzberg, 2012; Langmead et al., 2009) under default
489 parameters. bamCoverage in deepTools2 (Ramírez et al., 2016) was used to generate
490 bigwig coverage tracks in 50bp bins, with blacklisted regions from McMurchy et al. 2017
491 excluded, using the following parameters: -bs 50, --normalizeUsing RPKM (McMurchy et al.,
492 2017).
493 MACS2 (Feng et al., 2012; Zhang et al., 2008) default parameters were used to call
494 peaks and create bedgraph files for sequenced and mapped H3K36me3 ChIP samples and
495 input DNA samples with the following adjustments to account for H3K36me3 broader
496 domains: Broad-cutoff =0.001. Blacklisted regions from McMurchy et al. 2017 were
497 excluded for this analysis (McMurchy et al., 2017). Using published H3K36me3 modMine
498 Chip-chip called broad peaks (modENCODE_3555) from N2 L1 larvae as a guide, we then
499 merged called broad peaks within 1200bp using Bedtools: MergeBED (Quinlan and Hall,
500 2010). H3K9me2 bedgraph files used in our analysis were from a published dataset
501 (Rechtsteiner et al., 2019). Integrative Genome Viewer (IGV) was used to visualize
502 H3K36me3 reads normalized to reads per kilobase millions (RPKM) and H3K9me2 reads
503 normalized to 15 million reads (genome wide coverage of H3K9me2; Rechtsteiner et al.,
504 2019).
505 **RNAi methods.** RNAi by feeding was carried out using clones from the Ahringer library
506 (Kamath and Ahringer, 2003). Feeding experiments were performed on RNAi plates (NGM
507 plates containing 100 ug/ml ampicillin, 0.4mM IPTG, and 12.5ug/ml tetracycline). F0

508 worms were placed on RNAi plates as L2 larvae and then moved to fresh RNAi plates 48hrs
509 later where they were allowed to lay embryos for 2-4 hrs. F0 worms were then removed
510 from plates and sacrificed or placed in M9 buffer overnight so that starved L1 progeny
511 could be isolated for quantitative PCR (qPCR). F1 progeny were scored 72hrs after the
512 synchronized lay for developmental progression. For each RNAi experiment, *pos-1* RNAi
513 was used as a positive control. Each RNAi experiment reported here *pos-1* RNAi resulted in
514 >95% embryonic lethality, indicating that RNAi plates were optimal.
515 **Real-time expression analysis.** Total RNA was isolated using TRIzol reagent (Invitrogen)
516 from synchronized L1s born at room temperature (21°C – 22°C). cDNA synthesis and qPCR
517 were carried out as described (Kerr et al. 2014). All experiments were performed in
518 triplicate and normalized to *ama-1* mRNA expression (see Table S4 for primer sequences).
519 **Differential interference contrast microscopy.** Worms were immobilized in 0.1%
520 levamisole and placed on a 2% agarose pad for imaging at either 10x or 40x magnification.
521 40x DIC images were overlaid together using Adobe photoshop to generate high resolution
522 images of whole worms.

523 **Single Molecule Fluorescent *in situ* Hybridization (smFISH).** Quasar 570 labeled
524 smFISH probe sets for *htp-1* and *cpb-1* were designed using Stellaris Probe Designer
525 (Biosearch) (see Table S5 for probe sequences). The *htp-1* smFISH probes were designed
526 using the complete 1,059nt *htp-1* protein-coding sequence. Likewise, The *cpb-1* smFISH
527 probes were designed using the complete 1,683nt *cpb-1* protein-coding sequence. In
528 addition, an smFISH fluorescent probe set for *ama-1* was purchased from the DesignReady
529 catalog (cat#: VSMF-6002-5, Biosearch).

530 Synchronized L1 larvae for smFISH were obtained by bleaching 300-500 gravid
531 hermaphrodites and allowing embryos to hatch overnight on 6cm NGM plates lightly
532 seeded OP50 bacteria. L1 larvae were then washed into 1.5ul Eppendorf tubes using
533 nuclease-free M9 buffer. Fixation and hybridization steps followed the Stellaris RNA FISH
534 protocol for *C. elegans* adapted from RAJ lab protocol (Raj and Tyagi, 2010). In brief, we
535 resuspended L1 larvae in fixation buffer (3.7% formaldehyde in 1 x PBS) for 15 minutes at
536 room temperature then transferred tubes to liquid nitrogen. Samples were thawed in water
537 and placed on ice for 20 minutes. In our hands, we obtain better fluorescent signal by
538 freeze cracking L1 larvae. Following fixation, L1 Larvae were resuspended in 70% EtOH
539 and stored at 4°C for 24-48 hours. For all probe sets, we incubated L1 larvae in 100ul
540 hybridization buffer (containing 10% formamide and 125nm probe) for 4 hours at 37°C.
541 After hybridization, samples were washed in wash buffer at 37°C for 30 minutes, incubated
542 in 50ng/mL DAPI in wash buffer at 30°C for 30 minutes, washed once in 2x SSC for 2
543 minutes at room temperature, and mounted in Vectashield mounting medium. Mounted
544 slides were imaged immediately using a 100x objective on a spinning-disk confocal Nikon-
545 TiE imaging system. Images were captured using NIS-Elements software (Nikon) and
546 ImageJ (NIH, http://imagej.nih.gov/ij/) was used for viewing. ImageJ maximum projection
547 was used to project z-stack images to a single plane. The fluorescent intensity of smFISH
548 dots were > 2-fold above background as expected (Ji and van Oudenaarden, 2012).
549 **LET-858::GFP transgene silencing assay.** First generation *spr-5; met-2* hermaphrodites
550 were crossed to *let-858* transgenic males to generate *spr-5/+*; *met-2/+*; *let-858::gfp* animals.
551 The let-858 transgene is an extrachromosomal multicopy *let-858* array (Kelly and Fire,
552 1998). From these animals we generated *spr-5; met-2; let-858::gfp* animals and scored them

553 for somatic expression of LET-858::GFP using a standard stereoscope. L2 progeny from N2
554 and *spr-5; met-2* progeny expressing the LET-858::GFP transgene were scored as "bright"
555 (High level ubiquitous expression) , faint (barely visible and ubiquitous expression), or off
556 (no expression). Because less than 50% of progeny inherit the *let-858* transgene, we
557 normalized the percentage of progeny scored as "off" for LET-858::GFP to presence of the
558 *let-858* transgene based on genotyping for *gfp.* For N2, 0 out of 60 progeny that were
559 scored as "off" failed to inherit the *let-858* transgene indicating that the transgene is never
560 silenced in N2 progeny (data not shown, see Table S4 for primer sequences). For *spr-5;*
561 *met-2* progeny, 8 out of 50 progeny that were scored as "off" inherited the *let-858*
562 transgene indicating that the *let-858* transgene is completely silenced in some *spr-5; met-2*
563 progeny (data not shown).
564

565 **ACKNOWLEDGEMENTS**

566 We are grateful to members of the Katz lab, as well as T. Caspary and C. Bean, for their
567 helpful discussion and critical reading of the manuscript; M. J. Rowley for advice on
568 bioinformatics; S. Strome and L. Petrella for helpful discussion and experimental advice; D.
569 Lerit, R. Deal, V. Corces, and W. Kelly for the generous sharing of reagents and equipment.
570 We thank R. Horvitz, W. Kelly, and the *Caenorhabditis* Genetics Center (funded by NIH P40
571 OD010440) for strains. **Funding:** This work was funded by a grant to D.J.K. (NSF
572 IOS1931697); T.W.L. and B.S.C. were supported by the Fellowships in Research and Science
573 Teaching IRACDA postdoctoral program (NIH K12GM00680-15); and B.S.C. was also
574 supported by NIH F32 GM126734-01. **Author Contributions:** B.S.C. and D.J.K. conceived
575 and designed the study and wrote the manuscript. B.S.C. performed experiments under the

576 direction of D.J.K. B.S.C and D.J.K. analyzed data and interpreted results, with help from
577 T.W.L. J.S.B. initially performed *set-2* RNAi rescue experiment and C.F.P. initially performed
578 the *let-858* transgene silencing experiment. D.A.M. helped with RNA-seq analysis. All
579 authors discussed the results. **Data availability**: Raw and processed genomic data has
580 been deposited with the Gene Expression Omnibus (www.ncbi.nlm.nih.gov/geo) under
581 accession code GSE143839.
582

583 **Supplementary Material**

584 Figure supplements:

585 Figure 1: Supplemental Figure 1

586 Figure 2: Supplemental Figures 2 and 3

587 Figure 3: Supplemental Figure 4

588 Figure 4: Supplemental Figures 5 and 6

589 Supplementary tables 1-5

590

591 **REFERENCES**

592 Ancelin, K., Syx, L., Borensztein, M., Ranisavljevic, N., Vassilev, I., Briseño-Roa, L., Liu, T.,
593 Metzger, E., Servant, N., Barillot, E., Chen, C.-J., Schüle, R., Heard, E., 2016. Maternal
594 LSD1/KDM1A is an essential regulator of chromatin and transcription landscapes
595 during zygotic genome activation. Elife 5, 4615. doi:10.7554/eLife.08851
596 Batchelder, C., Dunn, M.A., Choy, B., Suh, Y., Cassie, C., Shim, E.Y., Shin, T.H., Mello, C.,
597 Seydoux, G., Blackwell, T.K., 1999. Transcriptional repression by the Caenorhabditis
598 elegans germ-line protein PIE-1. Genes Dev. 13, 202–212. doi:10.1101/gad.13.2.202
599 Bolger, A.M., Lohse, M., Usadel, B., 2014. Trimmomatic: a flexible trimmer for Illumina
600 sequence data. Bioinformatics 30, 2114–2120. doi:10.1093/bioinformatics/btu170
601 Brenner, S., 1974. The genetics of Caenorhabditis elegans. Genetics 77, 71–94.
602 Capowski, E.E., Martin, P., Garvin, C., Strome, S., 1991. Identification of grandchildless loci
603 whose products are required for normal germ-line development in the nematode
604 Caenorhabditis elegans. Genetics 129, 1061–1072.

605 Chen, E.Y., Tan, C.M., Kou, Y., Duan, Q., Wang, Z., Meirelles, G.V., Clark, N.R., Ma'ayan, A.,
606 2013. Enrichr: interactive and collaborative HTML5 gene list enrichment analysis tool.
607 BMC Bioinformatics 14, 128. doi:10.1186/1471-2105-14-128
608 Chong, J.X., Yu, J.-H., Lorentzen, P., Park, K.M., Jamal, S.M., Tabor, H.K., Rauch, A., Saenz, M.S.,
609 Boltshauser, E., Patterson, K.E., Nickerson, D.A., Bamshad, M.J., 2016. Gene discovery for
610 Mendelian conditions via social networking: de novo variants in KDM1A cause
611 developmental delay and distinctive facial features. Genet. Med. 18, 788–795.
612 doi:10.1038/gim.2015.161
613 Feng, J., Liu, T., Qin, B., Zhang, Y., Liu, X.S., 2012. Identifying ChIP-seq enrichment using
614 MACS. Nat Protoc 7, 1728–1740. doi:10.1038/nprot.2012.101
615 Fukuyama, M., Rougvie, A.E., Rothman, J.H., 2006. C. elegans DAF-18/PTEN mediates
616 nutrient-dependent arrest of cell cycle and growth in the germline. Curr. Biol. 16, 773–
617 779. doi:10.1016/j.cub.2006.02.073
618 Furuhashi, H., Takasaki, T., Rechtsteiner, A., Li, T., Kimura, H., Checchi, P.M., Strome, S.,
619 Kelly, W.G., 2010. Trans-generational epigenetic regulation of C. elegans primordial
620 germ cells. Epigenetics Chromatin 3, 15. doi:10.1186/1756-8935-3-15
621 Garvin, C., Holdeman, R., Strome, S., 1998. The phenotype of mes-2, mes-3, mes-4 and mes-
622 6, maternal-effect genes required for survival of the germline in Caenorhabditis
623 elegans, is sensitive to chromosome dosage. Genetics 148, 167–185.
624 Gu, Z., Eils, R., Schlesner, M., 2016. Complex heatmaps reveal patterns and correlations in
625 multidimensional genomic data. Bioinformatics 32, 2847–2849.
626 doi:10.1093/bioinformatics/btw313
627 Jambhekar, A., Dhall, A., Shi, Y., 2019. Roles and regulation of histone methylation in animal
628 development. Nat. Rev. Mol. Cell Biol. 20, 625–641. doi:10.1038/s41580-019-0151-1
629 Ji, N., van Oudenaarden, A., 2012. Single molecule fluorescent in situ hybridization
630 (smFISH) of C. elegans worms and embryos. WormBook 1–16.
631 doi:10.1895/wormbook.1.153.1
632 Kamath, R.S., Ahringer, J., 2003. Genome-wide RNAi screening in Caenorhabditis elegans.
633 Methods 30, 313–321. doi:10.1016/s1046-2023(03)00050-1
634 Katz, D.J., Edwards, T.M., Reinke, V., Kelly, W.G., 2009. A C. elegans LSD1 demethylase
635 contributes to germline immortality by reprogramming epigenetic memory. Cell 137,
636 308–320. doi:10.1016/j.cell.2009.02.015
637 Kelly, W.G., Fire, A., 1998. Chromatin silencing and the maintenance of a functional
638 germline in Caenorhabditis elegans. Development 125, 2451–2456.
639 Kerr, S.C., Ruppersburg, C.C., Francis, J.W., Katz, D.J., 2014. SPR-5 and MET-2 function
640 cooperatively to reestablish an epigenetic ground state during passage through the
641 germ line. Proc. Natl. Acad. Sci. U.S.A. 111, 9509–9514. doi:10.1073/pnas.1321843111
642 Kim, D., Langmead, B., Salzberg, S.L., 2015. HISAT: a fast spliced aligner with low memory
643 requirements. Nat. Methods 12, 357–360. doi:10.1038/nmeth.3317
644 Kim, J., Zhao, H., Dan, J., Kim, S., Hardikar, S., Hollowell, D., Lin, K., Lu, Y., Takata, Y., Shen, J.,
645 Chen, T., 2016. Maternal Setdb1 Is Required for Meiotic Progression and
646 Preimplantation Development in Mouse. PLoS Genet. 12, e1005970.
647 doi:10.1371/journal.pgen.1005970
648 Kim, J.-H., Lee, J.H., Lee, I.-S., Lee, S.B., Cho, K.S., 2017. Histone Lysine Methylation and
649 Neurodevelopmental Disorders. Int J Mol Sci 18, 1404. doi:10.3390/ijms18071404

650 Kreher, J., Takasaki, T., Cockrum, C., Sidoli, S., Garcia, B.A., Jensen, O.N., Strome, S., 2018.
651 Distinct Roles of Two Histone Methyltransferases in Transmitting H3K36me3-Based
652 Epigenetic Memory Across Generations in Caenorhabditis elegans. Genetics 210, 969–
653 982. doi:10.1534/genetics.118.301353
654 Kuleshov, M.V., Jones, M.R., Rouillard, A.D., Fernandez, N.F., Duan, Q., Wang, Z., Koplev, S.,
655 Jenkins, S.L., Jagodnik, K.M., Lachmann, A., McDermott, M.G., Monteiro, C.D., Gundersen,
656 G.W., Ma'ayan, A., 2016. Enrichr: a comprehensive gene set enrichment analysis web
657 server 2016 update. Nucleic Acids Res. 44, W90–7. doi:10.1093/nar/gkw377
658 Kurotaki, N., Imaizumi, K., Harada, N., Masuno, M., Kondoh, T., Nagai, T., Ohashi, H.,
659 Naritomi, K., Tsukahara, M., Makita, Y., Sugimoto, T., Sonoda, T., Hasegawa, T., Chinen,
660 Y., Tomita Ha, H.-A., Kinoshita, A., Mizuguchi, T., Yoshiura Ki, K.-I., Ohta, T., Kishino, T.,
661 Fukushima, Y., Niikawa, N., Matsumoto, N., 2002. Haploinsufficiency of NSD1 causes
662 Sotos syndrome. Nat. Genet. 30, 365–366. doi:10.1038/ng863
663 Langmead, B., Salzberg, S.L., 2012. Fast gapped-read alignment with Bowtie 2. Nat. Methods
664 9, 357–359. doi:10.1038/nmeth.1923
665 Langmead, B., Trapnell, C., Pop, M., Salzberg, S.L., 2009. Ultrafast and memory-efficient
666 alignment of short DNA sequences to the human genome. Genome Biol. 10, R25.
667 doi:10.1186/gb-2009-10-3-r25
668 Lederer, D., Grisart, B., Digilio, M.C., Benoit, V., Crespin, M., Ghariani, S.C., Maystadt, I.,
669 Dallapiccola, B., Verellen-Dumoulin, C., 2012. Deletion of KDM6A, a histone
670 demethylase interacting with MLL2, in three patients with Kabuki syndrome. Am. J.
671 Hum. Genet. 90, 119–124. doi:10.1016/j.ajhg.2011.11.021
672 Liao, Y., Smyth, G.K., Shi, W., 2014. featureCounts: an efficient general purpose program for
673 assigning sequence reads to genomic features. Bioinformatics 30, 923–930.
674 doi:10.1093/bioinformatics/btt656
675 Love, M.I., Huber, W., Anders, S., 2014. Moderated estimation of fold change and dispersion
676 for RNA-seq data with DESeq2. Genome Biol. 15, 550. doi:10.1186/s13059-014-0550-8
677 McMurchy, A.N., Stempor, P., Gaarenstroom, T., Wysolmerski, B., Dong, Y., Aussianikava, D.,
678 Appert, A., Huang, N., Kolasinska-Zwierz, P., Sapetschnig, A., Miska, E.A., Ahringer, J.,
679 2017. A team of heterochromatin factors collaborates with small RNA pathways to
680 combat repetitive elements and germline stress. Elife 6, 7931. doi:10.7554/eLife.21666
681 Mello, C.C., Draper, B.W., Krause, M., Weintraub, H., Priess, J.R., 1992. The pie-1 and mex-1
682 genes and maternal control of blastomere identity in early C. elegans embryos. Cell 70,
683 163–176. doi:10.1016/0092-8674(92)90542-k
684 Passannante, M., Marti, C.-O., Pfefferli, C., Moroni, P.S., Kaeser-Pebernard, S., Puoti, A.,
685 Hunziker, P., Wicky, C., Müller, F., 2010. Different Mi-2 complexes for various
686 developmental functions in Caenorhabditis elegans. PLoS ONE 5, e13681.
687 doi:10.1371/journal.pone.0013681
688 Quinlan, A.R., Hall, I.M., 2010. BEDTools: a flexible suite of utilities for comparing genomic
689 features. Bioinformatics 26, 841–842. doi:10.1093/bioinformatics/btq033
690 Raj, A., Tyagi, S., 2010. Detection of individual endogenous RNA transcripts in situ using
691 multiple singly labeled probes. Meth. Enzymol. 472, 365–386. doi:10.1016/S0076-
692 6879(10)72004-8
693 Ramírez, F., Ryan, D.P., Grüning, B., Bhardwaj, V., Kilpert, F., Richter, A.S., Heyne, S., Dündar,
694 F., Manke, T., 2016. deepTools2: a next generation web server for deep-sequencing data
695 analysis. Nucleic Acids Res. 44, W160–5. doi:10.1093/nar/gkw257

696 Rayasam, G.V., Wendling, O., Angrand, P.-O., Mark, M., Niederreither, K., Song, L., Lerouge, T.,
697 Hager, G.L., Chambon, P., Losson, R., 2003. NSD1 is essential for early post-implantation
698 development and has a catalytically active SET domain. EMBO J. 22, 3153–3163.
699 doi:10.1093/emboj/cdg288
700 Rechtsteiner, A., Costello, M.E., Egelhofer, T.A., Garrigues, J.M., Strome, S., Petrella, L.N.,
701 2019. Repression of Germline Genes in Caenorhabditis elegans Somatic Tissues by
702 H3K9 Dimethylation of Their Promoters. Genetics 212, 125–140.
703 doi:10.1534/genetics.118.301878
704 Rechtsteiner, A., Ercan, S., Takasaki, T., Phippen, T.M., Egelhofer, T.A., Wang, W., Kimura, H.,
705 Lieb, J.D., Strome, S., 2010. The histone H3K36 methyltransferase MES-4 acts
706 epigenetically to transmit the memory of germline gene expression to progeny. PLoS
707 Genet. 6, e1001091. doi:10.1371/journal.pgen.1001091
708 Seydoux, G., Mello, C.C., Pettitt, J., Wood, W.B., Priess, J.R., Fire, A., 1996. Repression of gene
709 expression in the embryonic germ lineage of C. elegans. Nature 382, 713–716.
710 doi:10.1038/382713a0
711 Shi, Y., Lan, F., Matson, C., Mulligan, P., Whetstine, J.R., Cole, P.A., Casero, R.A., Shi, Y., 2004.
712 Histone demethylation mediated by the nuclear amine oxidase homolog LSD1. Cell 119,
713 941–953. doi:10.1016/j.cell.2004.12.012
714 Shi, Y.-J., Matson, C., Lan, F., Iwase, S., Baba, T., Shi, Y., 2005. Regulation of LSD1 histone
715 demethylase activity by its associated factors. Mol. Cell 19, 857–864.
716 doi:10.1016/j.molcel.2005.08.027
717 Strome, S., 2005. Specification of the germ line. WormBook 1–10.
718 doi:10.1895/wormbook.1.9.1
719 Sulston, J.E., Schierenberg, E., White, J.G., Thomson, J.N., 1983. The embryonic cell lineage of
720 the nematode Caenorhabditis elegans. Dev. Biol. 100, 64–119. doi:10.1016/0012-
721 1606(83)90201-4
722 Tunovic, S., Barkovich, J., Sherr, E.H., Slavotinek, A.M., 2014. De novo ANKRD11 and KDM1A
723 gene mutations in a male with features of KBG syndrome and Kabuki syndrome. Am. J.
724 Med. Genet. A 164A, 1744–1749. doi:10.1002/ajmg.a.36450
725 Unhavaithaya, Y., Shin, T.H., Miliaras, N., Lee, J., Oyama, T., Mello, C.C., 2002. MEP-1 and a
726 homolog of the NURD complex component Mi-2 act together to maintain germline-
727 soma distinctions in C. elegans. Cell 111, 991–1002.
728 Wasson, J.A., Simon, A.K., Myrick, D.A., Wolf, G., Driscoll, S., Pfaff, S.L., Macfarlan, T.S., Katz,
729 D.J., 2016. Maternally provided LSD1/KDM1A enables the maternal-to-zygotic
730 transition and prevents defects that manifest postnatally. Elife 5, 296.
731 doi:10.7554/eLife.08848
732 Wingett, S.W., Andrews, S., 2018. FastQ Screen: A tool for multi-genome mapping and
733 quality control. F1000Res 7, 1338. doi:10.12688/f1000research.15931.2
734 Xu, Q., Xiang, Y., Wang, Q., Wang, L., Brind'Amour, J., Bogutz, A.B., Zhang, Y., Zhang, B., Yu, G.,
735 Xia, W., Du, Z., Huang, C., Ma, J., Zheng, H., Li, Y., Liu, C., Walker, C.L., Jonasch, E.,
736 Lefebvre, L., Wu, M., Lorincz, M.C., Li, W., Li, L., Xie, W., 2019. SETD2 regulates the
737 maternal epigenome, genomic imprinting and embryonic development. Nat. Genet. 51,
738 844–856. doi:10.1038/s41588-019-0398-7
739 Zhang, Y., Liu, T., Meyer, C.A., Eeckhoute, J., Johnson, D.S., Bernstein, B.E., Nusbaum, C.,
740 Myers, R.M., Brown, M., Li, W., Liu, X.S., 2008. Model-based analysis of ChIP-Seq (MACS).
741 Genome Biol. 9, R137. doi:10.1186/gb-2008-9-9-r137

Figure 1. *spr-5; met-2* mutants display severe developmental delay. 10x Differential Interference Contrast (DIC) images of N2 (A), *spr-5* (B), *met-2* (C), and *spr-5; met-2* progeny (D) 72 hours post synchronized lay. Scale bar: 100µm. (E) Percentage of N2, *spr-5*, *met-2*, and *spr-5; met-2* progeny that reached the adult stage (% Adult Progeny) by 72 hours post synchronized lay. Error bars represent the standard deviation of the mean from three experiments.

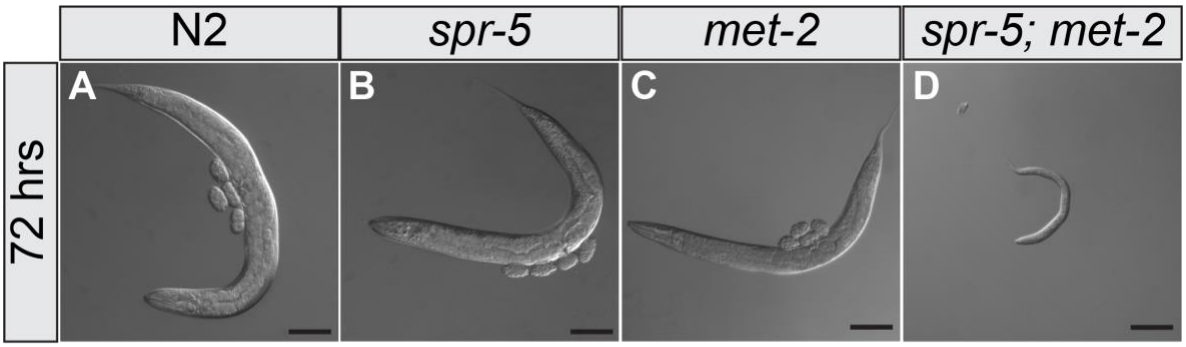

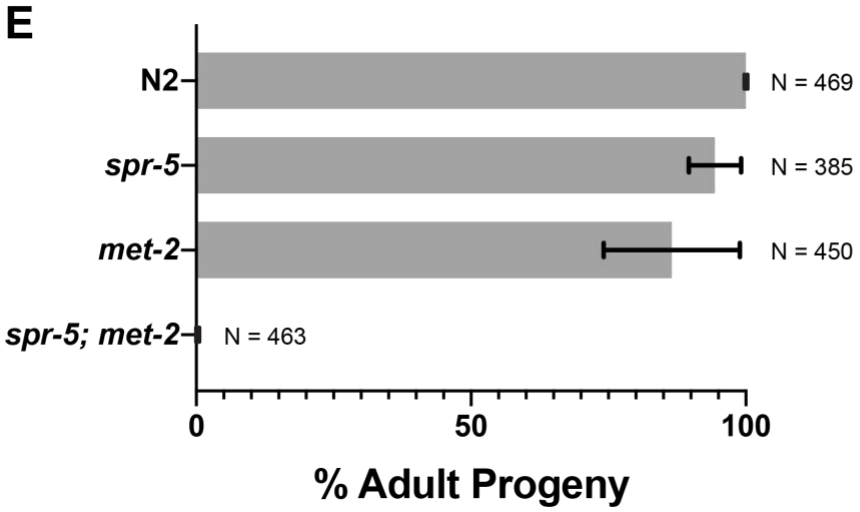

Figure 2. MES-4 germline genes are ectopically expressed in *spr-5; met-2* mutant soma. Overlap between MES-4 germline genes and genes up-regulated (A) and down-regulated (B) in *spr-5; met-2* L1 progeny. Significant over-enrichment in A was determined by the hypergeometric test (*P-value < 4.34e-20). (C) Heatmap of log2 fold change (FC) of 176 MES-4 germline genes in *spr-5, met-2* and *spr-5; met-2* mutants compared to N2. log2FC values are represented in a yellow to blue gradient and range from -2 to 5. Yellow represents genes with negative log2FC values and blue represents genes with positive log2FC values compared to N2. The remaining 21 MES-4 germline genes were not included because they do not have an expression value in one or more of the data sets (*spr-5*, *met-2,* or *spr-5; met-2*)

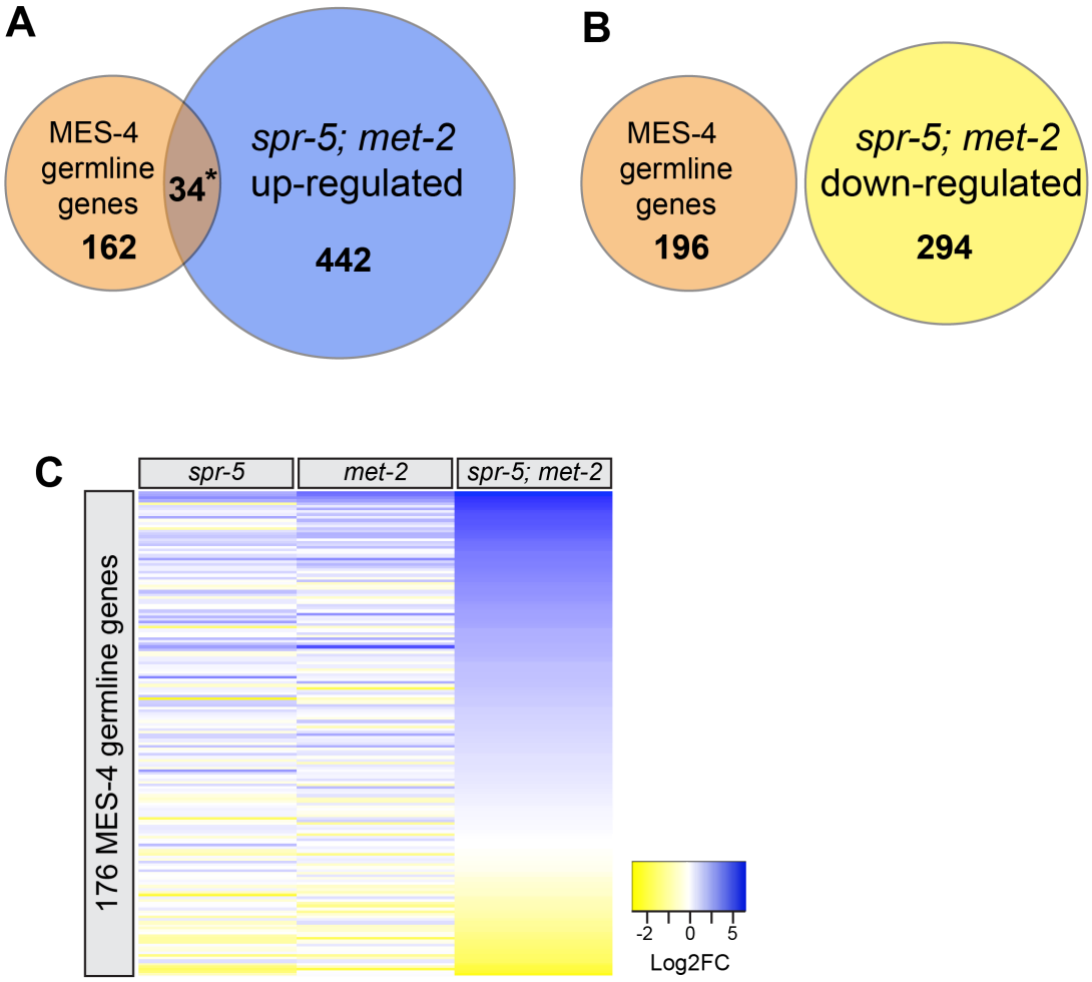

Figure 3. *spr-5; met-2* L1 progeny ectopically express MES-4 germline genes in multiple somatic tissues. 40x smFISH images of *htp-1* (A, C, D, F) and *cpb-1* (G, I, J, L) endogenous mRNAs in N2 (A-C, G-I) and *spr-5; met-2* (D-F, J-L) L1 progeny. DAPI was used as a nuclear marker (B, C, E, F, H, I, K, L). Insets are high magnification images of the germ cells, Z2 and Z3, in N2 L1 progeny. Arrows (J, L) denote ectopic *cpb-1* mRNA foci in somatic cells. Scale bar 40µm.

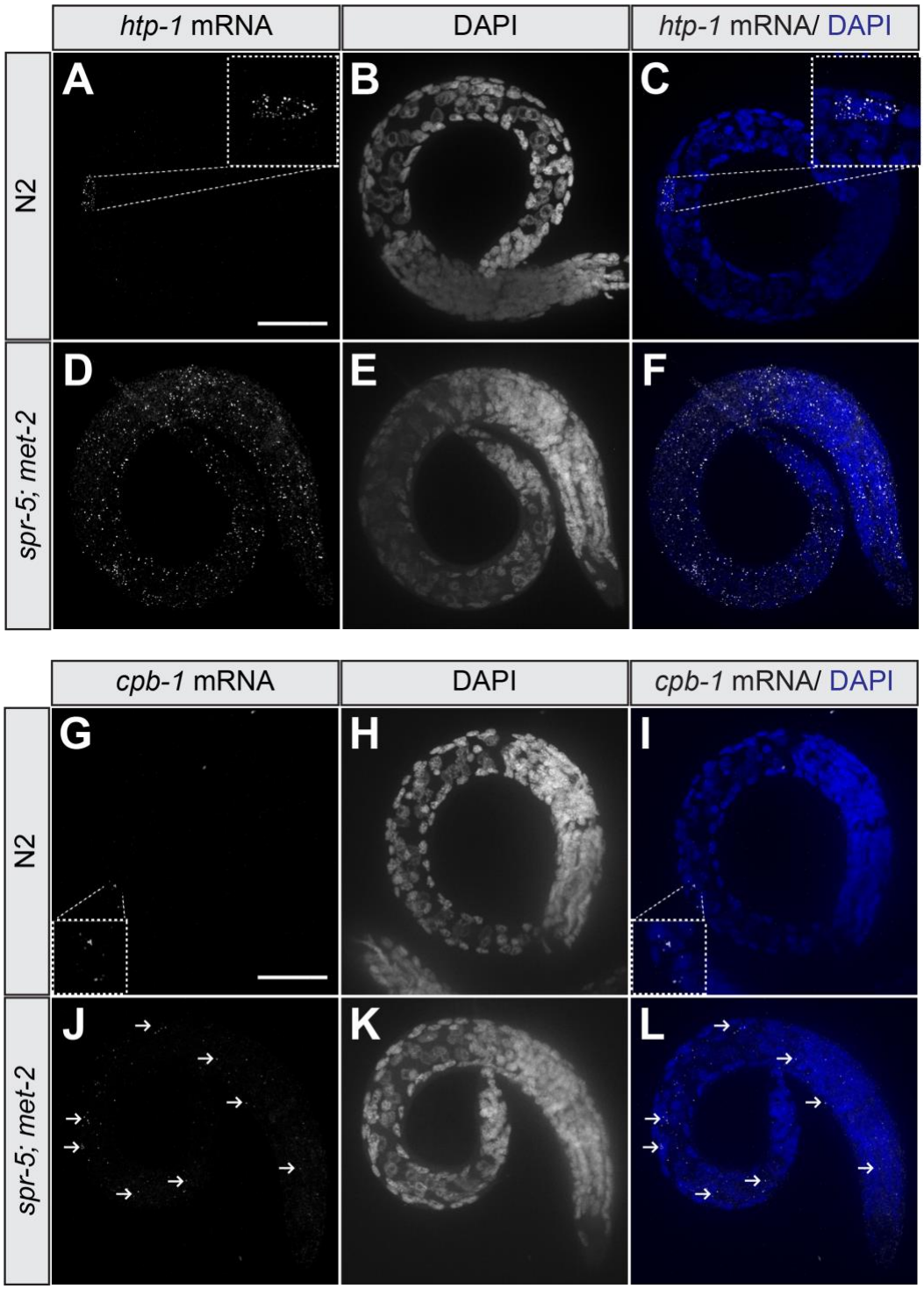

Figure 4. MES-4 germline genes display ectopic H3K36me3 in *spr-5; met-2* L1 progeny. Heatmap of H3K36me3 ChIP-seq reads normalized to reads per kilobase million (RPKM) over the gene bodies of 196 MES-4 germline genes in wild-type (N2) (A) versus *spr-5; met-2* (B) L1 progeny (second replicate in Figure S5). Gene bodies were pseudoscaled to 1kb with 500bp borders separated by orange bars that represent the transcriptional start site (TSS) and transcriptional end site (TES). Integrative Genome Viewer (IGV) image of H3K36me3 ChIP-seq reads normalized to RPKM at MES-4 germline genes (C-F, J-M) and control genes (G-I, N-P) in N2 (C-I) versus *spr-5; met-2* (J-P) L1 progeny. RPKM IGV windows were scaled between 0 and 202 RPKM for all genes.

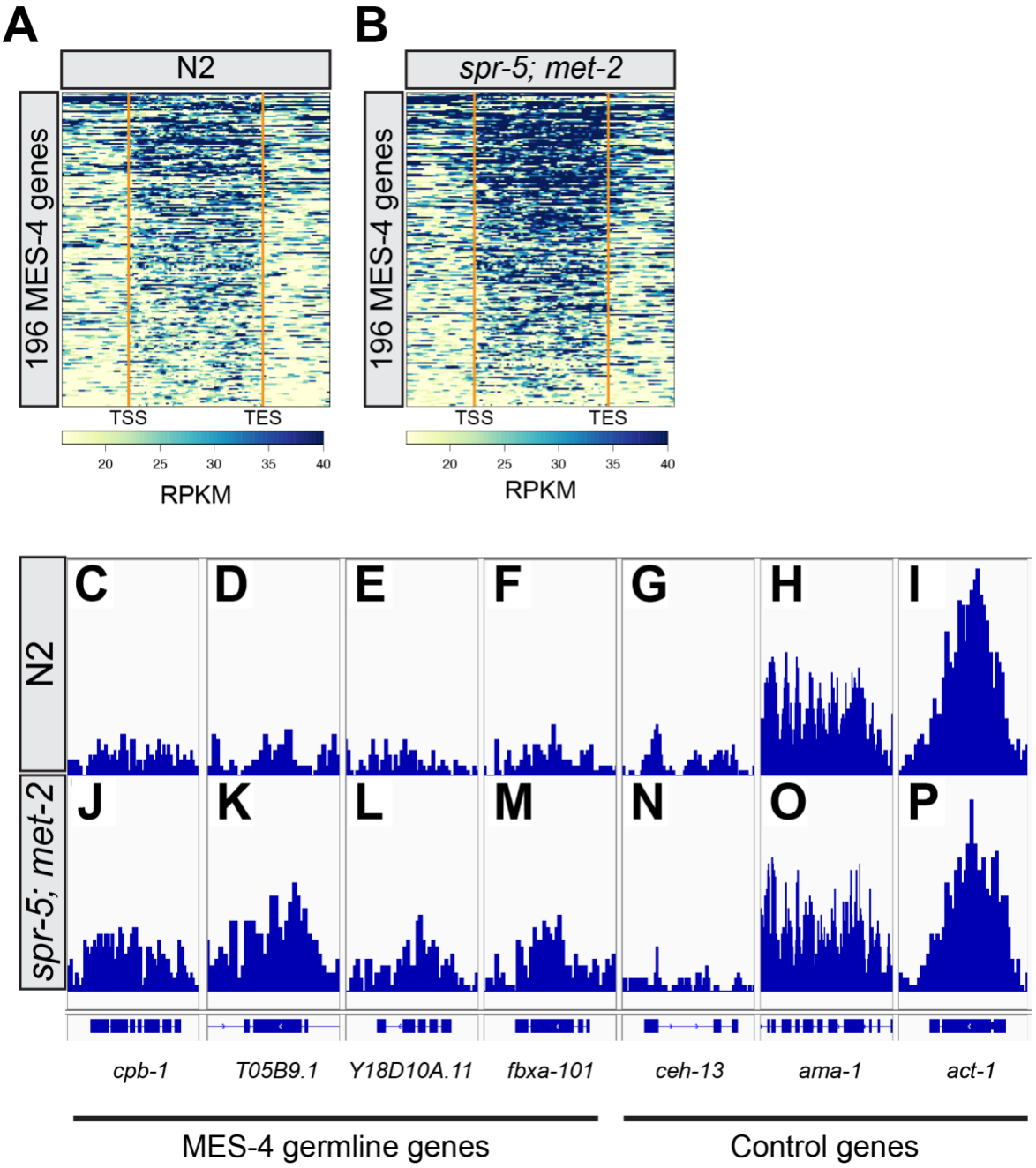

Figure 5. Knocking down MES-4 rescues ectopic expression of MES-4 germline genes in *spr-5; met-2* L1 progeny. Quantitative RT-PCR showing the relative units of expression for nine MES-4 germline genes (*cpb-1, csr-1*, *fbxa-101*, *htp*-1, *T05B9.1*, *Y18D10A.11*, *ftr-1*, *rmh-1*, *K12D12.5*) in L1 progeny of *spr-5; met-2* hermaphrodites fed either control L4440 RNAi (grey bars) or *mes-4* RNAi (black bars) versus N2 fed control L4440 RNAi (white bars). Relative units of expression from two biological replicates (R1 and R2) were calculated for each gene by averaging triplicate RT_PCR reactions and normalizing to a control gene, *ama-1*. Error bars represent the standard error of the mean (SEM) for triplicate RT_PCR reactions. For all nine genes, *mes-4* RNAi significantly reduced the relative expression of *spr-5; met-2* compared to *spr-5; met-2* fed L4440 control RNAi (t-test, p-value <0.001).

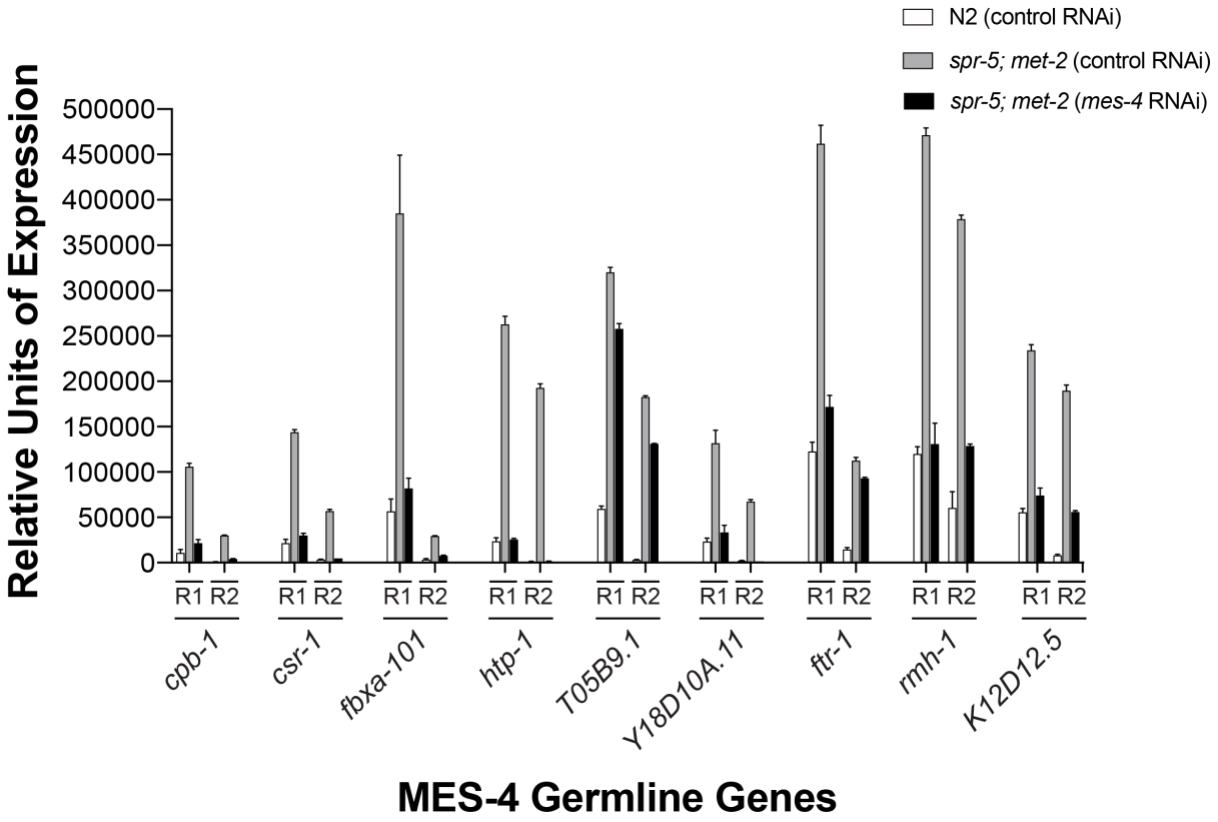

Figure 6. Knocking down MES-4 rescues developmental delay in *spr-5; met-2* progeny. DIC images of N2 (A-D) or *spr-5; met-2* (E-H) progeny from hermaphrodite parents treated with control (L4440 vector only) RNAi (A, E), *mes-4* RNAi (B, F), *met-1*RNAi (C, G), or *set-2* RNAi (D, H) 72 hours post synchronized lay. Scale bar: 100µm. (I) Quantification of the number of progeny (represented as % Adult Progeny) from A-H that made it to adults by 72 hours. Error bars represent the standard deviation of the mean from two or three experiments. N represents the total number of progeny scored across independent experiments. (t-test, **** represent a p-value <0.0001).

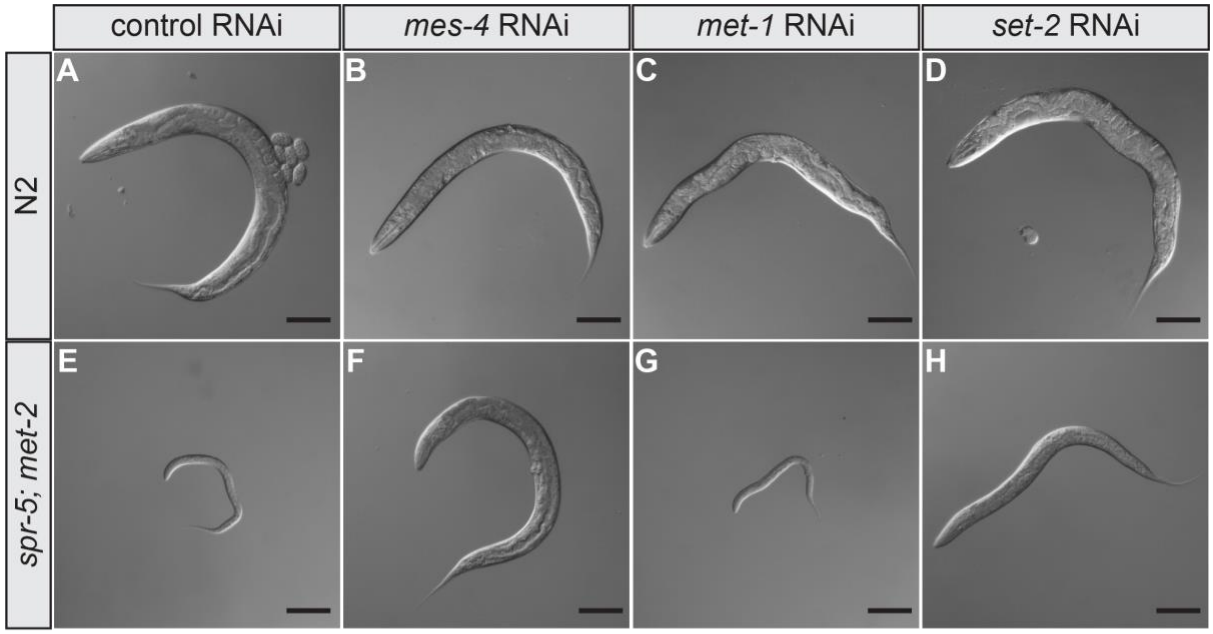

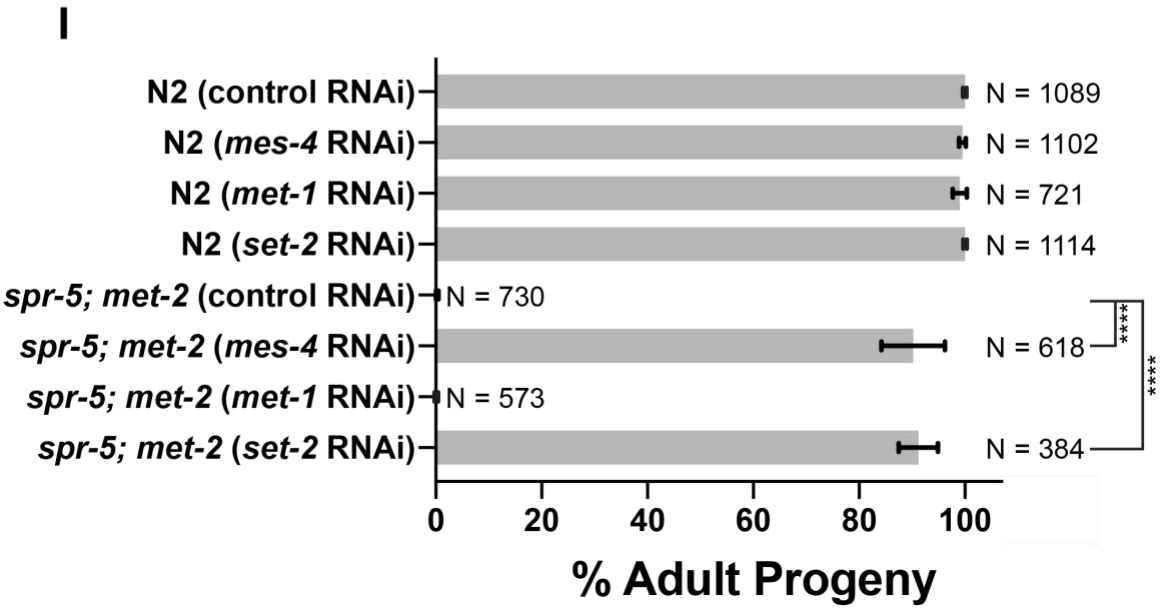

Figure 7. *let-858* transgene silencing in the soma of *spr-5; met-2* mutants. 40x differential contrasting interference (DIC) (A, C, E, G, and I) and immunofluorescent (B, D, F, H, and J) images of N2 (A-D) and *spr-5; met-2* (E-J) L2 progeny. Arrows denote faint expression of LET-858::GFP. Scale bar: 50 μm. Scale bar is the same for all panels. Percentage of animals where the expression level of LET-858::GFP was scored as either bright expressing (bright green, representative shown in panel B and F), faint expressing (dark green, representative shown in panel D and H), or not expressing (black, representative shown in panel J) in N2 (N=132) versus *spr-5; met-2* (N=87) progeny (K). The quantification represents the percentages of LET-858::GFP expressing progeny from two independent experiments. To control for the segregation of the *let-858* transgene, progeny scored as "off" were normalized for the presence of the *let-858* transgene in animals as detected by PCR (see methods).

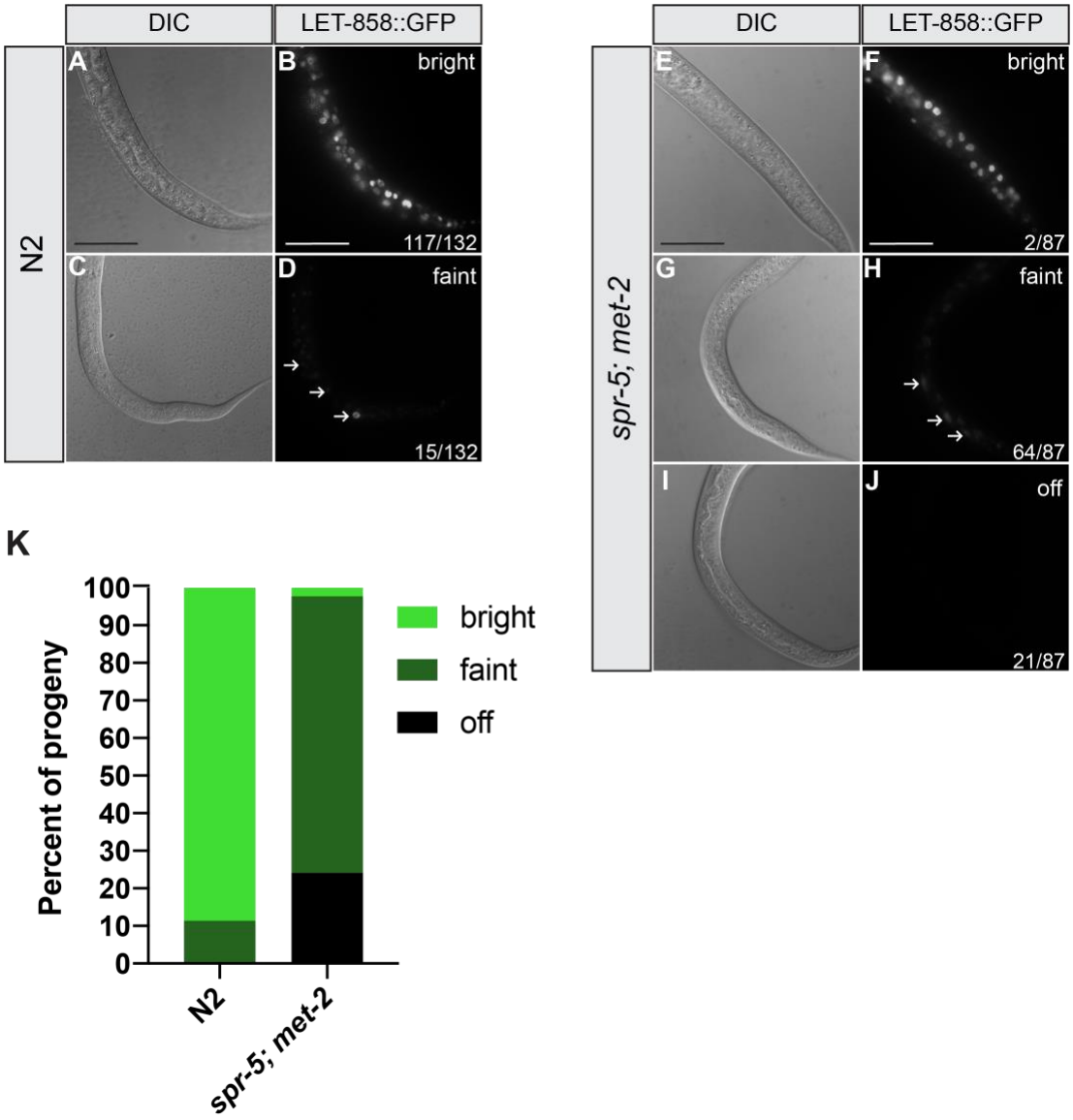

Figure 8: A model for how maternal reprogramming of inherited histone methylation helps to specify germline versus soma. During development, the COMPASS Complex and MET-1 add transcriptionally coupled H3K4me1/2 and H3K36me2/3 to germline expressed genes in the parental germline. (A) At fertilization, these germline expressed genes undergo maternal epigenetic reprogramming by SPR-5 and MET-2 to remove H3K4me1/2 and add H3K9me1/2. In the germline blastomeres of the embryo, PIE-1 prevents global transcription by inhibiting Pol II. In the absence of transcription, MES-4 maintains H3K36me2/3 at MES-4 germline genes that have acquired transcriptionally coupled H3K36me2/3 in the previous germline. This ensures that these genes remain bookmarked for re-expression once the germline begins to proliferate later in development. (B) Without SPR-5 and MET-2 maternal reprogramming, H3K4me1/2 is inappropriately inherited in somatic tissues, allowing MES-4 to ectopically add H3K36me2/3 at these germline genes. This leads to ectopic expression of MES-4 germline genes in somatic tissues and a severe developmental delay. Orange circles represent somatic cells, Grey circles outlined in blue dashed-lines represent germ cells, and orange circles outlined in dashed-blue lines depict somatic cells that ectopically express MES-4 germline genes. P-lineage, germline blastomeres, are indicated by the letter P, and the primordial germline cells are indicated by Z2 and Z3.

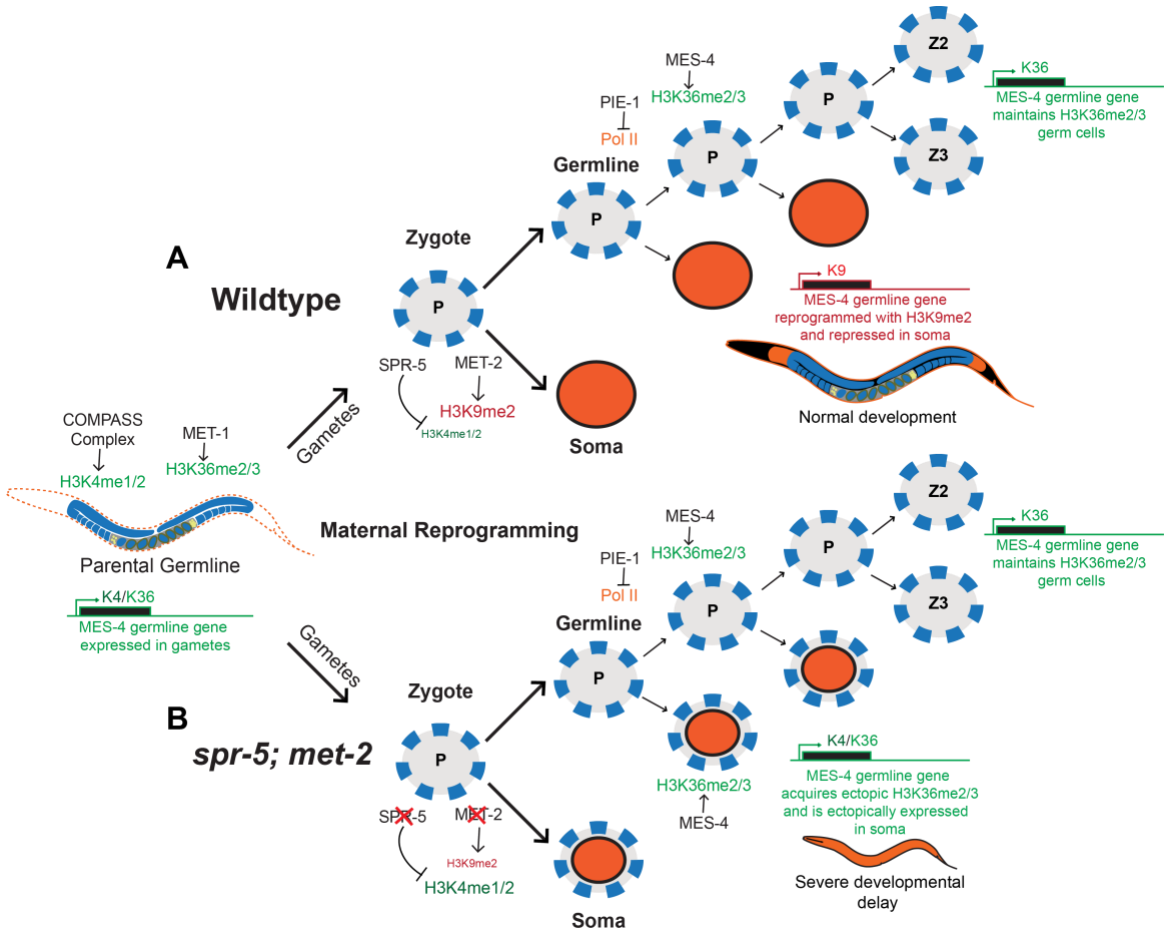

Supplemental Figure 1. *spr-5; met-2* mutants display severe developmental delay and protruding vulva. 40x DIC images of N2 (A), *spr-5* (B), *met-2* (C), and *spr-5; met-2* (D) progeny at 72 hours post synchronized lay. DIC image in (D) was magnified an additional 4x. 40x DIC images of two examples of *spr-5; met-2* adult progeny (E, F) at seven days post synchronized lay. Dashed-line (D) outlines germline and asterisks (E, F) denote protruding vulva. Scale bar: 100µm. (G) Quantification of *spr-5; met-2* progeny that reached the adult stage by seven days post synchronized lay, along with quantification of protruding vulva (Pvl) in these animals that reached the adult stage. The 876 progeny scored came from a total of 25 hermaphrodites across two independent experiments.

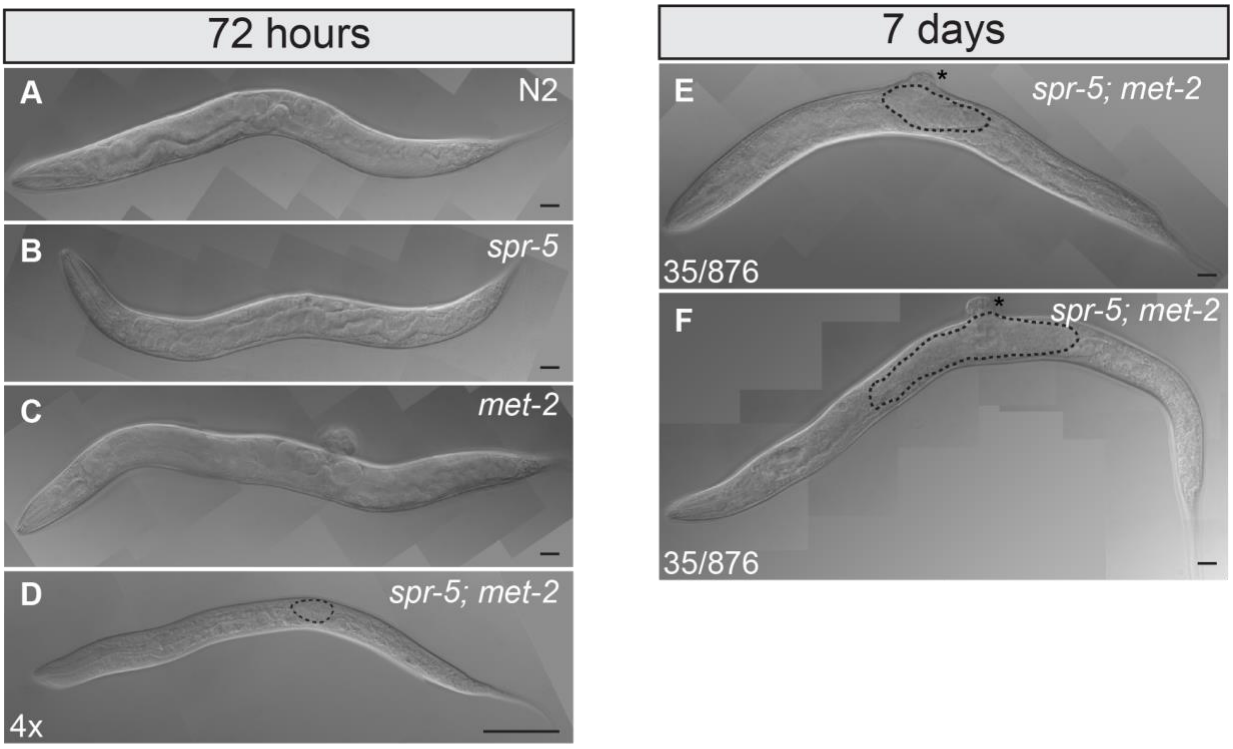

G

Total # of progeny scored	Total # of adult progeny	Percent of adult progeny	Total # of adult progeny with Pvl	Percent of adult progeny with Pvl
876	35	3.9%	31	88.5%

Supplemental Figure 2: Differential gene expression in *spr-5, met-2, and spr-5; met-2* progeny *compared* to N2 progeny. (A) Table summary of differentially expressed genes in *spr-5, met-2, and spr-5; met-2* L1 progeny from DeSEQ2 analysis (significance cut-off of p< 0.05). (B) Overlap of differentially expressed genes between *spr-5, met-2, and spr-5; met-2* L1 progeny. Gene Ontology analysis showing Biological Processes (C) and Cellular Components (D) amongst genes that were up-regulated (red) and down-regulated (green) in *spr-5; met-2* L1 progeny compared to N2. Combined Score was computed to determine gene set enrichment (Chen et al., 2013).

A

Genotype	Total # of differentially expressed genes	Up-regulated > 2 fold log2 FC	Down-regulated < 2 fold log2 FC
spr-5	343	142	41
met-2	413	146	67
spr-5; met-2	778	476	294

B

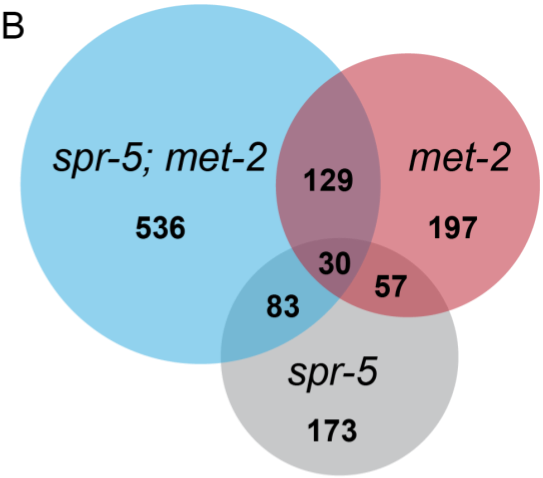

C

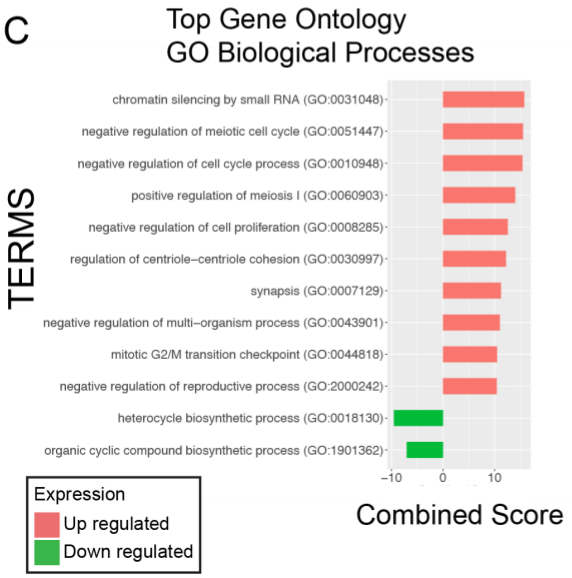

D

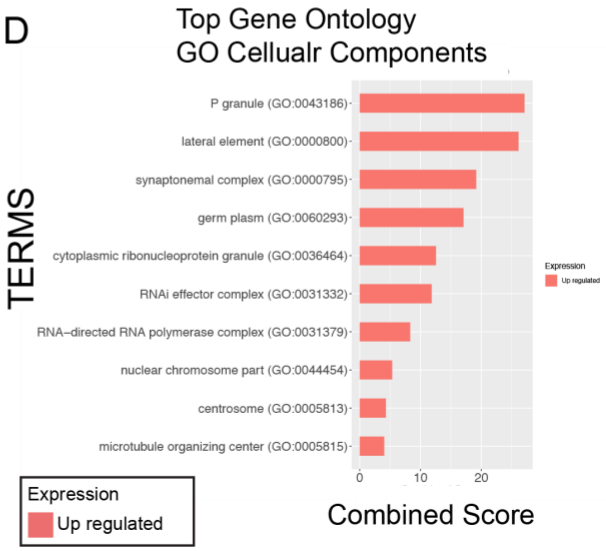

Supplemental Figure 3. Differential expression and replicate comparison of RNAseq experiments performed on N2, *spr-5*; *met-2*, and *spr-5; met-2* L1 progeny. Volcano plot of log2 fold changes in gene expression (x-axis) by statistical significance (-Log$_{10}$ P-value; y-axis) in *spr-5* (A), *met-2* (B), and *spr-5; met-2* (C) L1 Progeny compared to N2. Heatmap of differentially expressed RNA-seq transcripts between N2 and *spr-5* (D), *met-2* (E), and *spr-5; met-2* (F). Data was scaled and hierarchical clustering was performed using the complete linkage algorithm. Instead of Euclidean distance, distance was measured by calculating pairwise distance. Higher (red) and lower (green) expression is reported as a z-score.

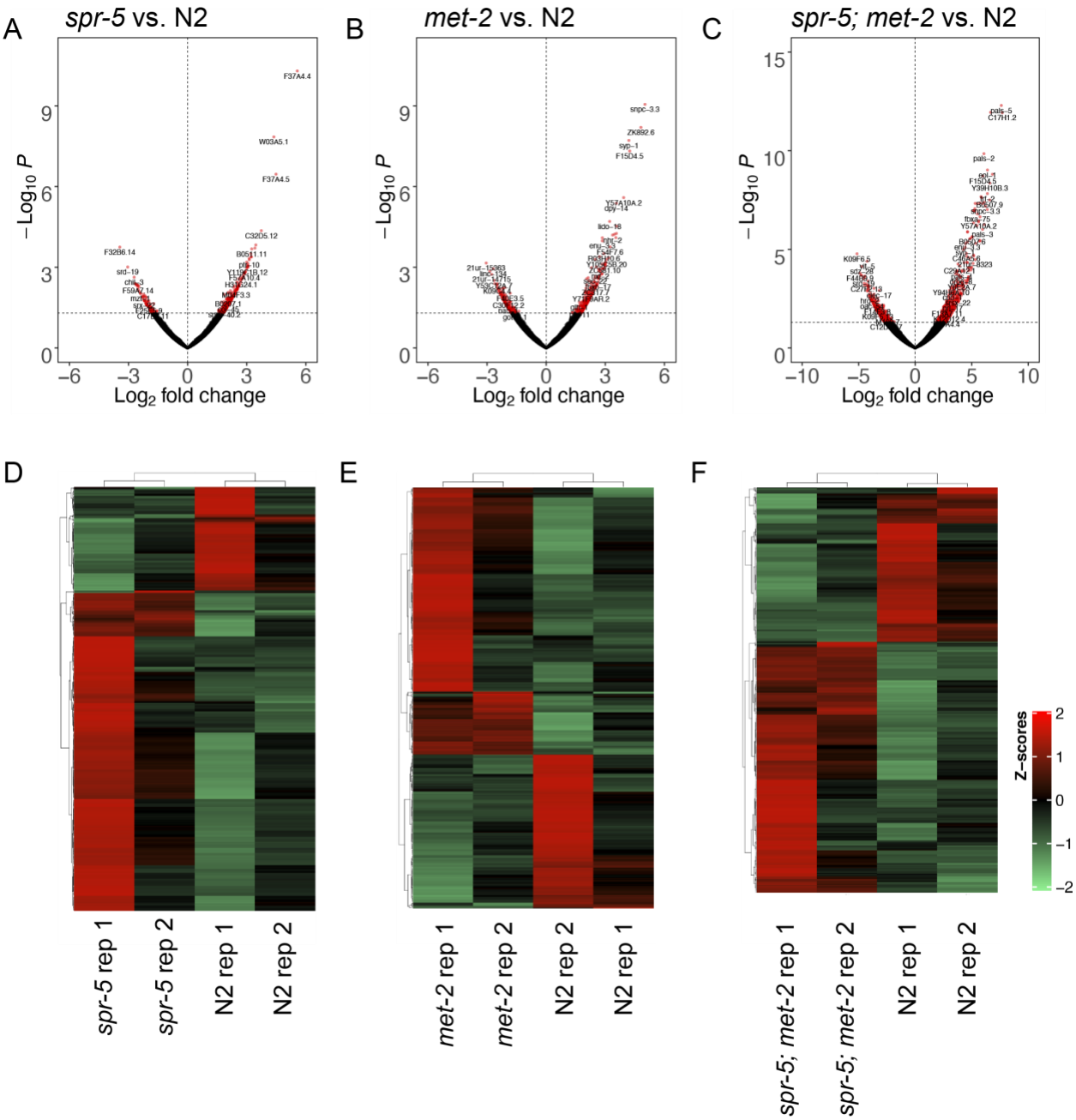

Supplemental Figure 4. smFISH control experiments. smFISH images of *ama-1* mRNA (A, C, D, F) and a no probe control (G, I, J, L) in N2 (A-C, G-I) and *spr-5; met-2* (D-F, J-L) L1 progeny. DAPI was used as a nuclear marker (B, C, E, F, H, I, K, L). Scale bar 40µm.

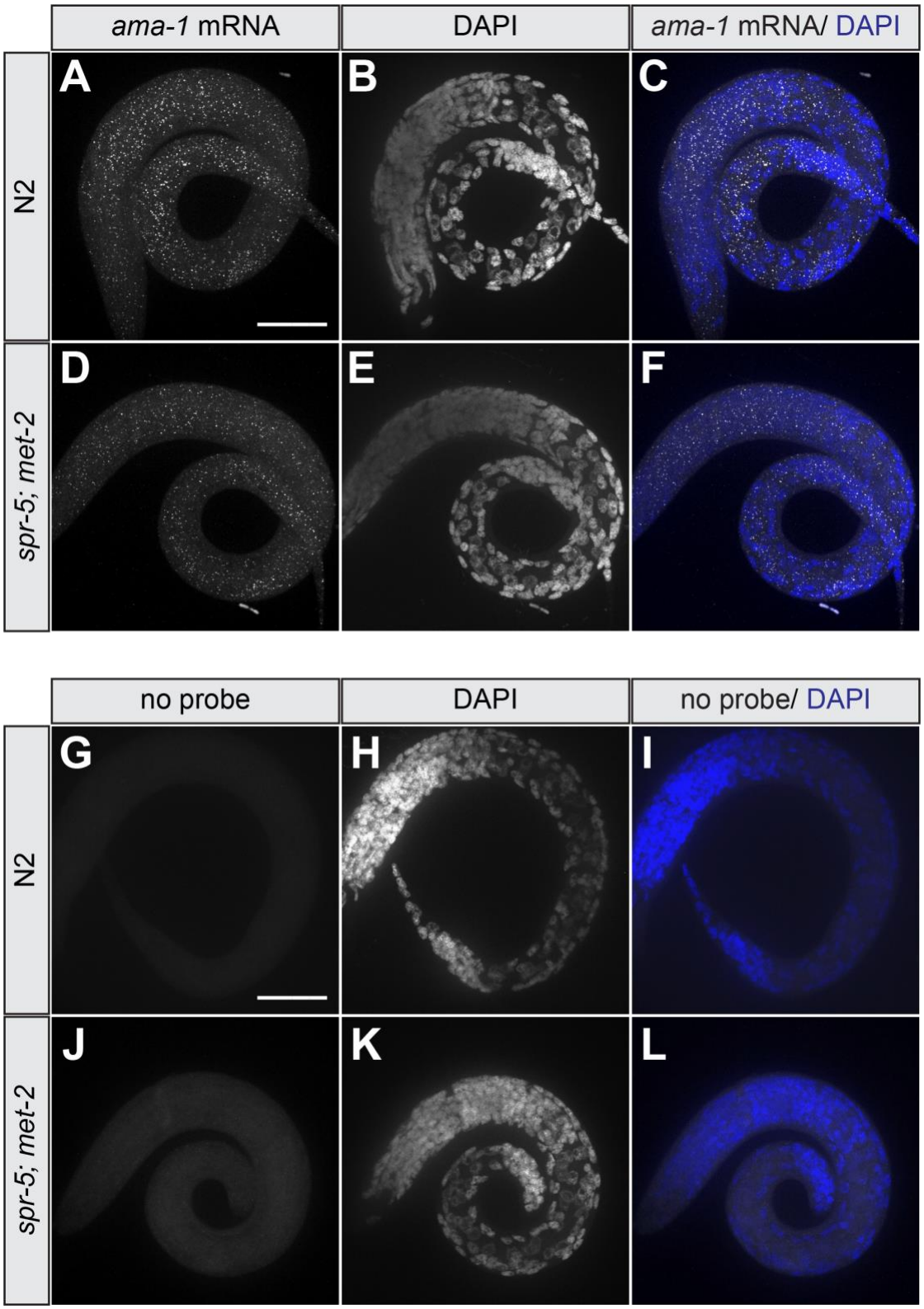

Supplemental Figure 5: Replicate comparison of H3K36me3 ChIP-seq analysis in *spr-5; met-2* L1 progeny. Heatmap of H3K36me3 ChIP-seq reads from a second replicate (1st replicate in Figure 4) normalized to reads per kilobase million (RPKM) over the gene bodies of 196 MES-4 germline genes in wild-type (N2) (A) versus *spr-5; met-2* (B) L1 progeny. Gene bodies were pseudoscaled to 1kb with 500bp borders separated by orange bars that represent the transcriptional start site (TSS) and transcriptional end site (TES). Integrative Genome Viewer (IGV) image of H3K36me3 ChIP-seq reads from replicate 2 normalized to RPKM at MES-4 germline genes (C-F, J-M) versus control genes (G-I, N-P) in N2 (C-I) and *spr-5; met-2* (J-P) L1 progeny. RPKM IGV windows were scaled between 0 and 107 RPKM for all genes. Venn-diagram displaying the overlap of H3K36me3 ChIP-seq called broad peaks for N2 (Q) and *spr-5; met-2* (R) replicates.

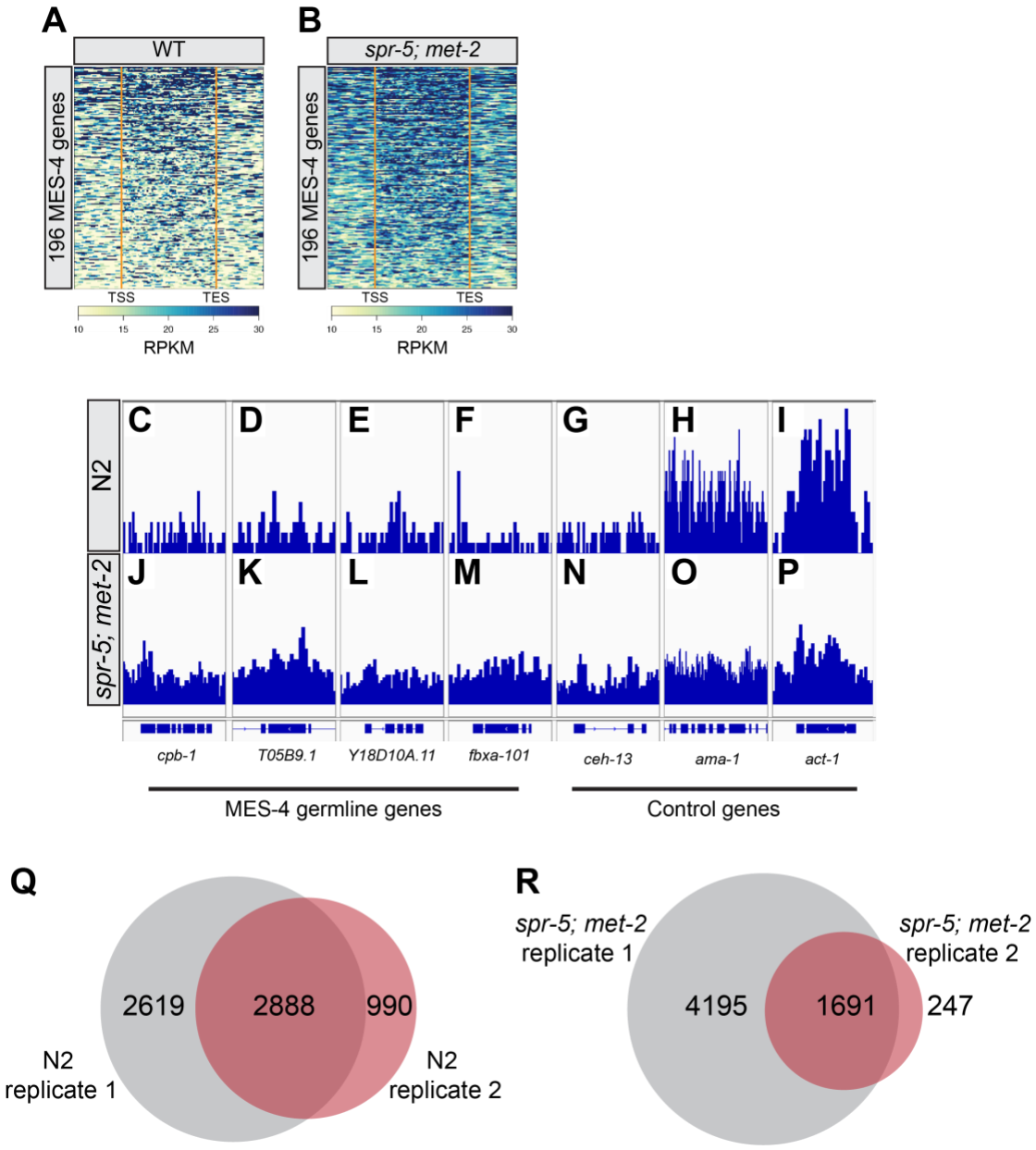

Supplemental Figure 6: MES-4 germline genes display H3K9me2 at their promoters. Heatmap of H3K9me2 promoter peaks in N2 L1 progeny at all 196 MES-4 germline genes (A), and at the 34 MES-4 germline genes that were ectopically expressed in the soma of *spr-5; met-2* progeny (B). ChIP-seq reads were scaled to genome wide coverage for H3K9me2 (15 million reads). The transcriptional start site (TSS) is denoted by an orange bar with 500bp flanking regions upstream and downstream of the TSS. Integrative Genome Viewer (IGV) image of ChIP-seq reads from N2 L1 progeny scaled to genome wide coverage for H3K9me2 (15 million reads) over the promoters of MES-4 germline genes that were ectopically expressed in the soma of *spr-5; met-2* progeny (C-F) and control genes (G-I). IGV windows were scaled between 0 and 255 RPKM. Asterisks (*) denotes H3K9me2 promoter peaks at MES-4 germline genes.

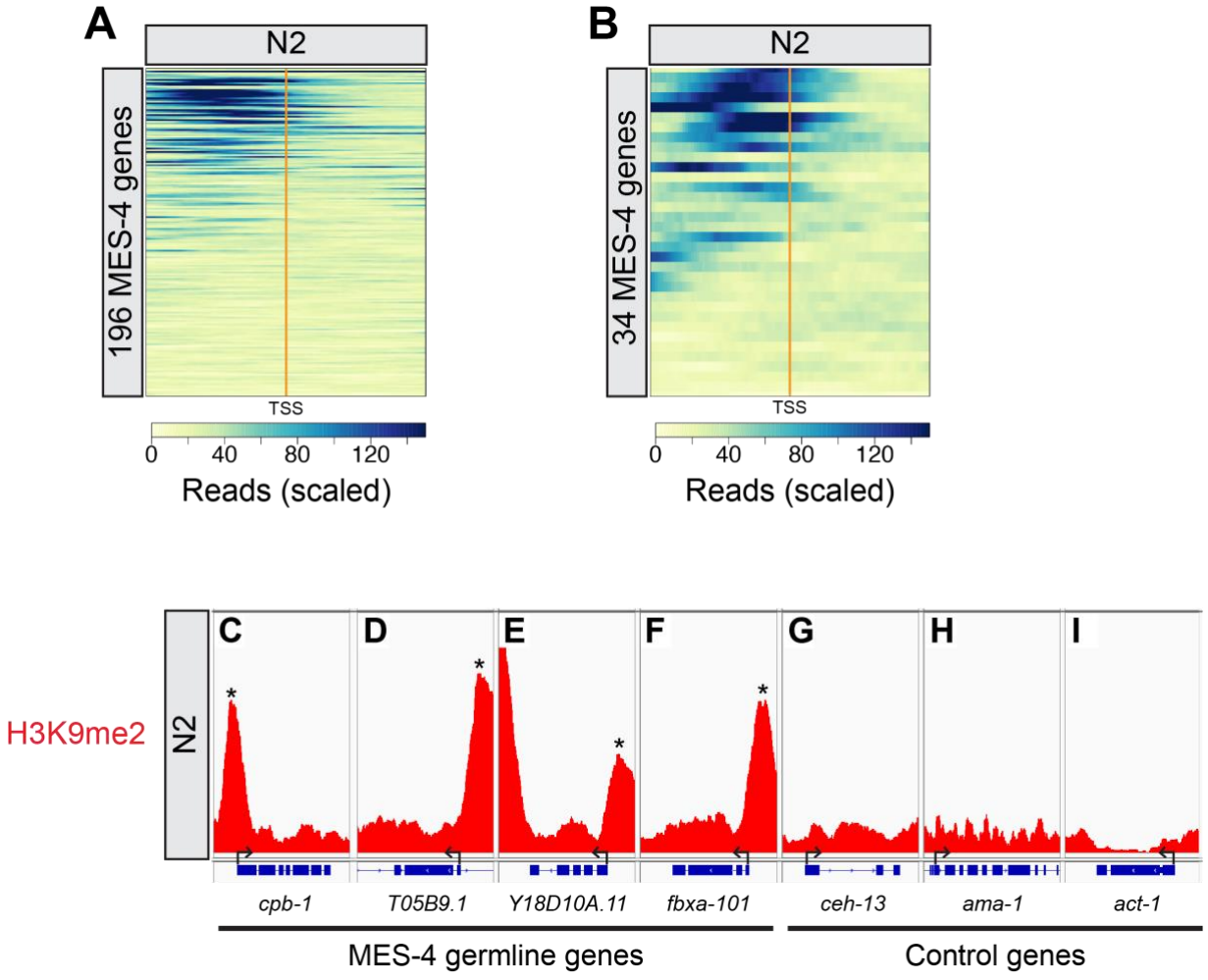

Supplemental Table S1. Raw scores for developmental delay in N2, *spr-5*, *met-2*, and *spr-5; met-2* progeny (see Figure 1A-E). Progeny were scored 72 hours after a synchronized lay as developing to the L1, L2, L3, L4, or young adult (YA) stage. N represents the total number of progeny scored in each experiment.

Supplemental Table S2. List of differentially expressed transcripts (P<0.05) in *spr-5*, *met-2* and *spr-5; met-2* L1 progeny compared to N2 progeny from DESeq2 analysis.

Supplemental Table S3. List of 176 MES-4 germline gene log2(FC) values used to generate heatmap (see Figure 2C) in *spr-5, met-2, and spr-5; met-2* L1 progeny compared to N2 progeny from DESeq2 analysis.

Supplemental Table S4: List of primer sequences used for genotyping and RT-PCR.

Supplemental Table S5: List of probe sequences for *htp-1* and *cpb-1* used in smFISH experiments.